COMSOL CONFERENCE 2015 GRENOBLE

UNIVERSITA' DEGLI STUDI DI ROMA TorVergata

Multiphysics Design of a Klystron Buncher

Alberto Leggieri, Davide Passi, Giovanni Saggio and Franco Di Paolo

Department of Electronic Engineering, University of Rome "Tor Vergata"
alberto.leggieri@uniroma2.it

EH Frontier
Expanding High-frequency Frontier

Outline

- Introduction
- Operative principles
- Motivations
- Buncher Features
- Numerical model
- Simulation Results
- Conclusions

Outline

- Introduction
- Operative principles
- Motivations
- Buncher Features
- Numerical model
- Simulation Results
- Conclusions

Introduction

3 GHz Klystron

91 GHz Klystron

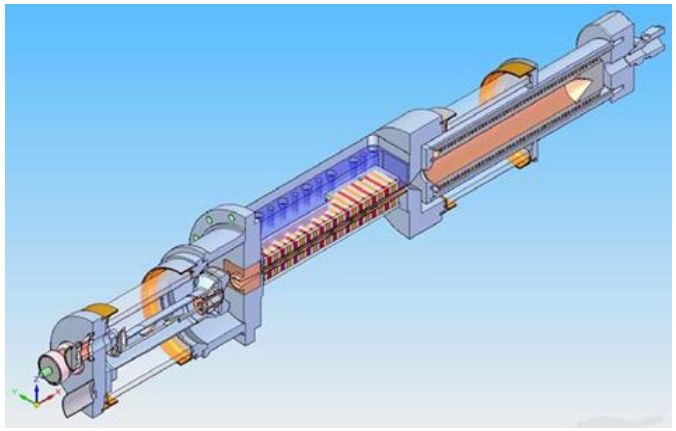

Microfabrication

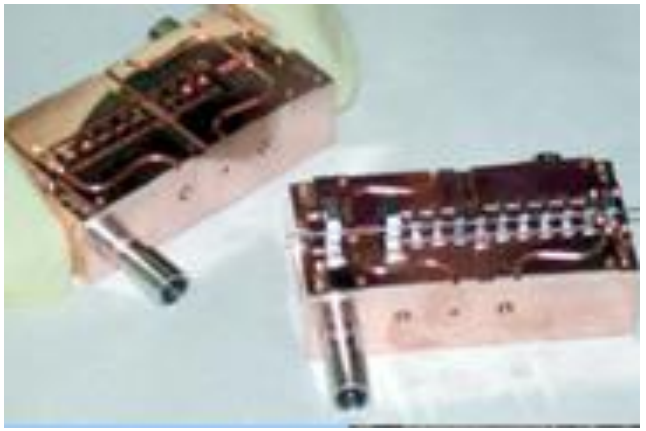

Millimetric wave applications for high power, around the Kilowatt, employees vacuum tube technology. Klystron and TWT are the most diffused devices for broad band applications. Klystrons are well known vacuum tube amplifier employing a set of resonant cavities as grids and may be developed through several interesting solutions and can operate around 100 GHz.
In millimeter and sub-millimeter wave frequency bands, solid-state devices present lack of performances, overcome by vacuum tubes, especially by Klystrons employing cold cathodes.

Introduction

Multiphysics-based model Design

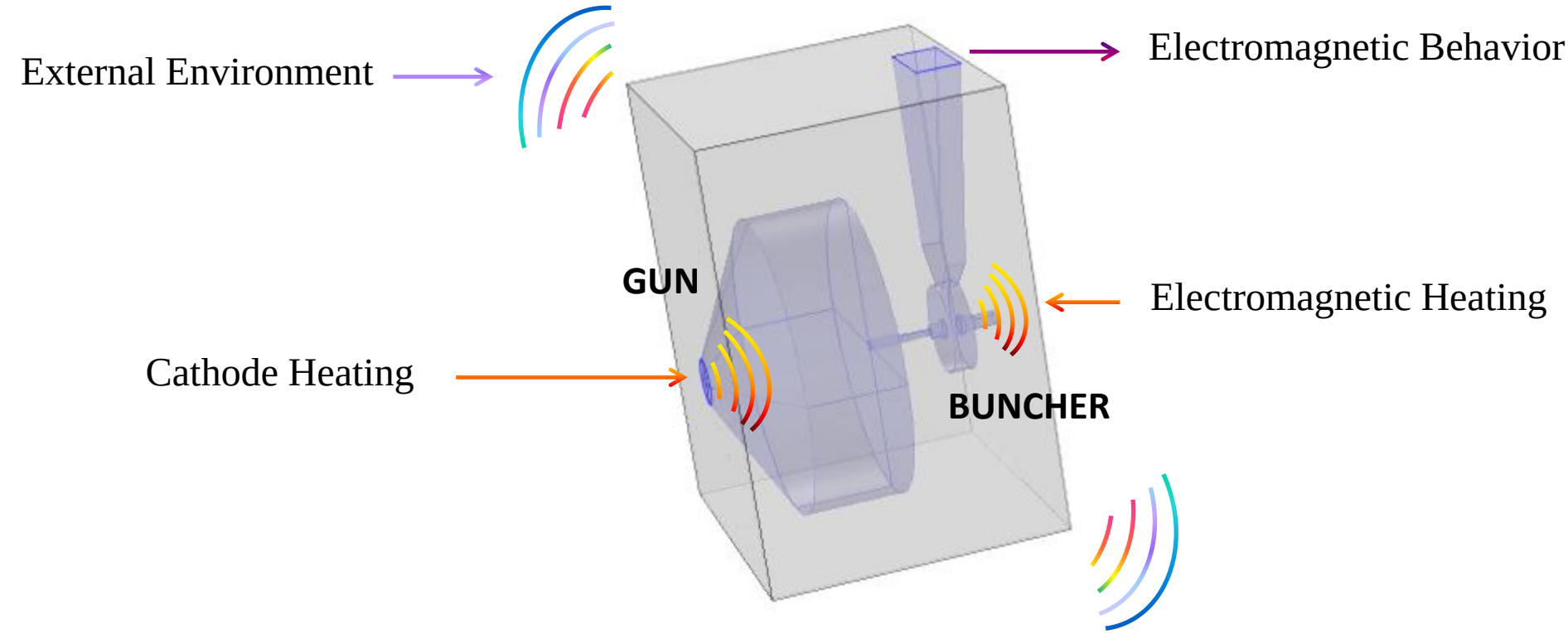

A computational model of a **Buncher cavity for millimetric klystron** following a **Multiphysics approach** is proposed in this paper. At these narrow dimensions, the device is critically exposed to multiple physics effects, due to the power dissipations and external environment, influencing the electromagnetic performances. **The cavity is integrated with a carbon nanotube cold cathode** in order to reduce thermal expansion and cooled by an opportune **airflow** that regulates the temperature distribution to **compensate the resonant frequency shift**.

Outline

- Introduction
- Operative principles
- Motivations
- Buncher Features
- Numerical model
- Simulation Results
- Conclusions

Introduction

ELECTRON MICROSCOPE

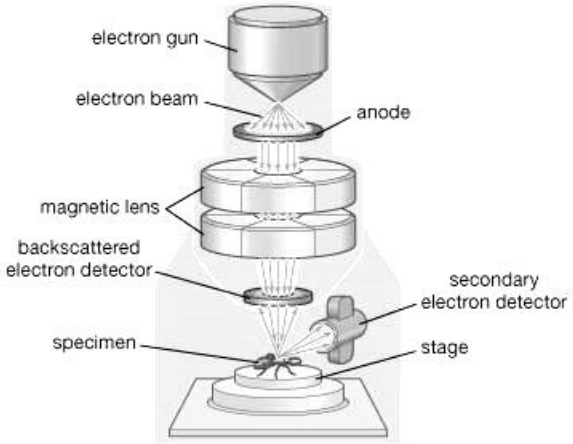

TWT

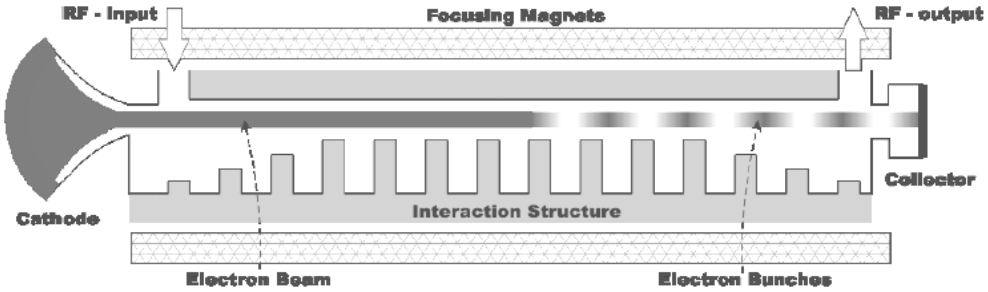

KLYSTRON

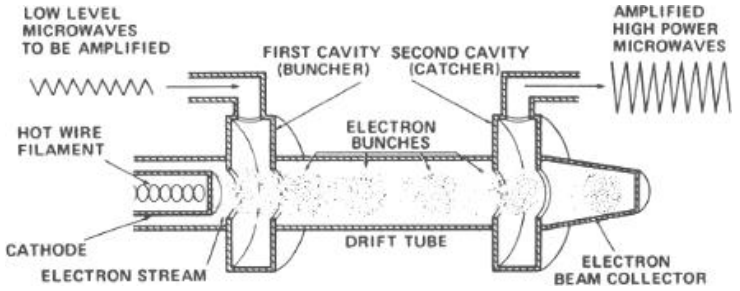

LINEAR ACCELERATOR

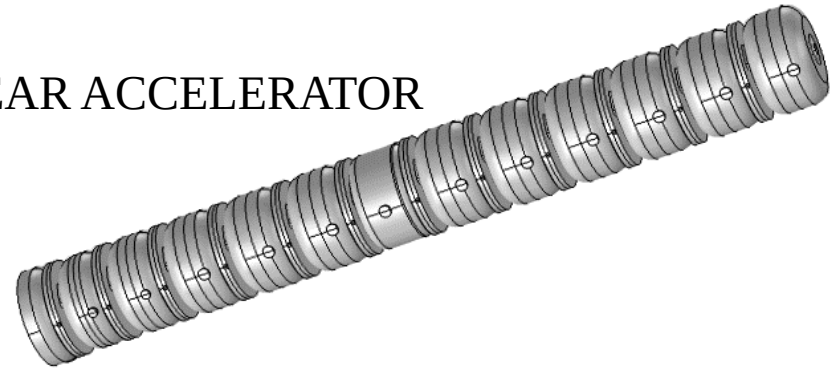

In many applications **very small beam dimension** are required as sub-millimeter waves vacuum tubes, electromagnetic environmental instrumentation and electron microscopes for spatial applications.

Vacuum tubes employ **electron gun's** as sources for the main electron current to be manipulated in the tube.

Operative principles

Cathode Electron Emission

Thermionic emission

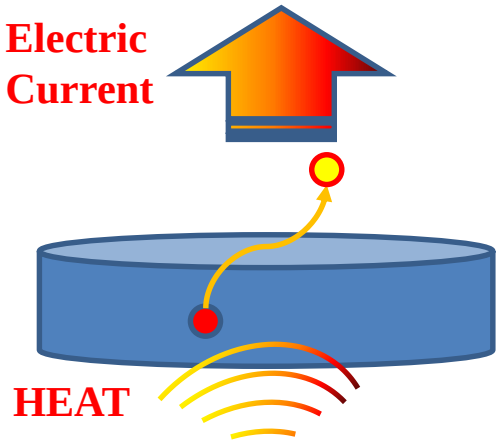

Photo-electric emission

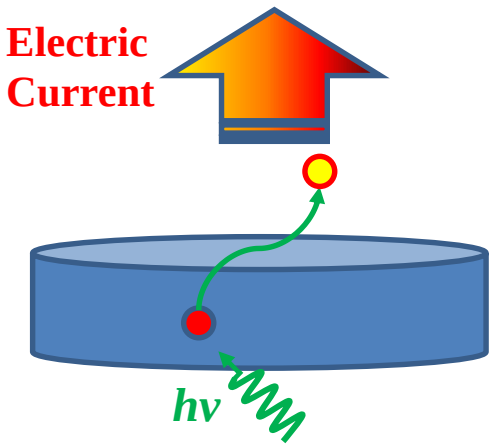

Field emission

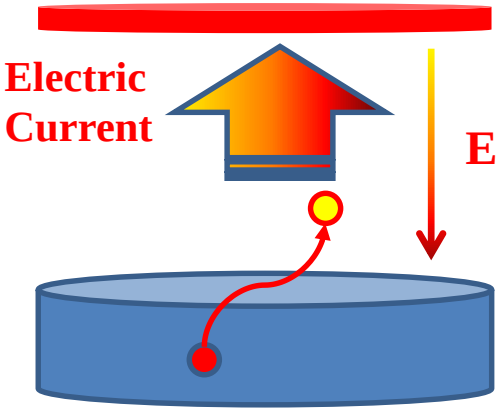

Electron emission can occur under three fundamental processes:

1. Thermionic emission, obeying the Richardson-Dushmann law: Thermal excitation allows free electrons reaching the vacuum level and escape the material.

2. Photo-electric emission obeying the Spicer Model: Photon absorption by the electron, Electron transport to the surface (electron scattering and phonon interaction with lattice atoms may reduce emission), Escape through the barrier (only electrons traveling toward the cathode surface, i.e. electron's momentum perpendicular to the surface can be emitted).

3. Field emission, following Fowler-Nordheim law: A very high fields (10^9 V/m or more) lowers the barrier in order to allow electrons quantum mechanically tunnel through the barrier.

Operative principles

CNT Cold Cathode: Field emission

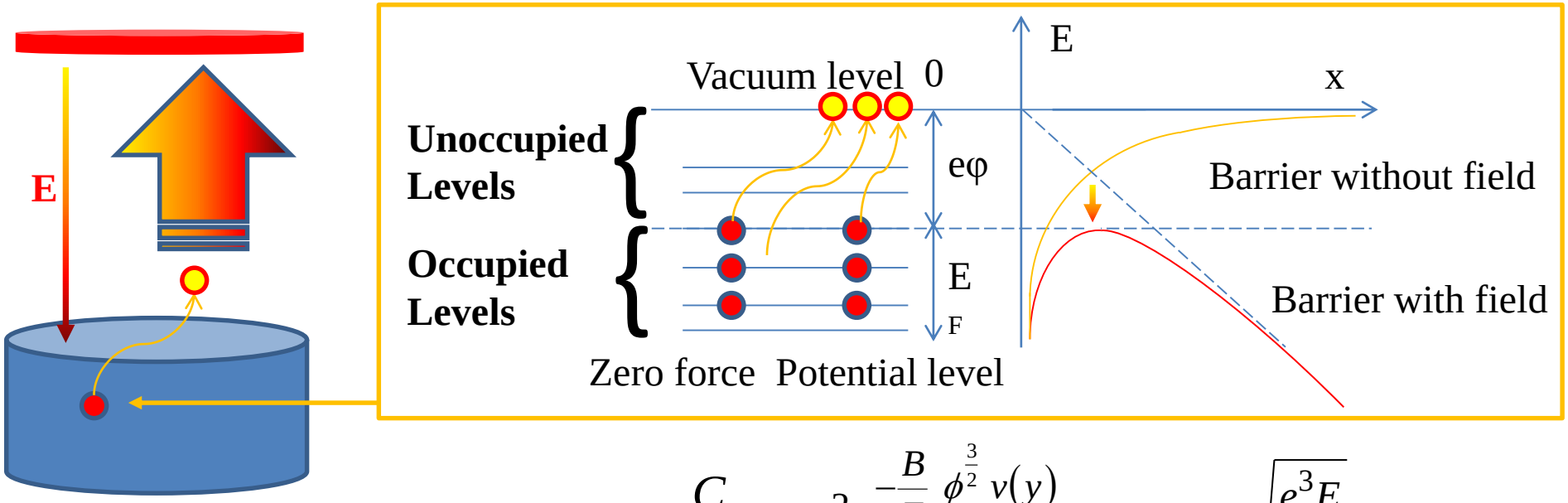

Fowler-Nordheim Law

$$J = \frac{C}{\phi\, t^2(y)} E^2 e^{-\frac{B}{E}\phi^{\frac{3}{2}} v(y)} \qquad y = \sqrt{\frac{e^3 E}{\phi^2}}$$

The electron source employed in this study is a carbon nanotube (CNT) emitter array. While an external electric field is applied, it changes the potential of cathode surface into a reduced potential barrier with a finite width. This effects is known as the Schottky effect. If the field is high enough, particles can tunnel through the barrier. This is called field emission and is regulated by the Fowler and Nordheim law where E is the applied electric field, Φ is the work function of the metal, C and B are constants of the material, and v(y) and t(y) are functions which arise due the inclusion of image charge effects and are near unity for typical conditions.

Operative principles

CNT Cold Cathode: Advantages of Cold Cathodes

- Working at ambient temperature
- Cathode patterning
- Small dimensions
- Possibility of modulate emitted current

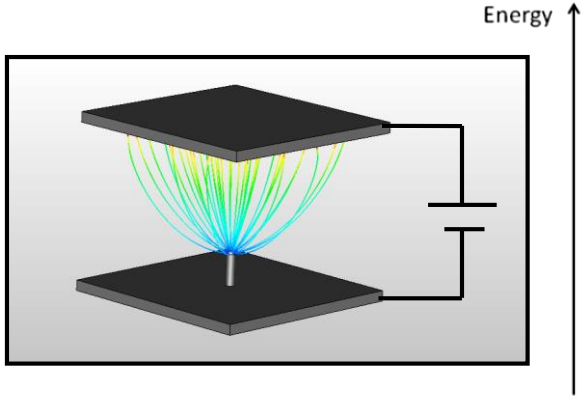

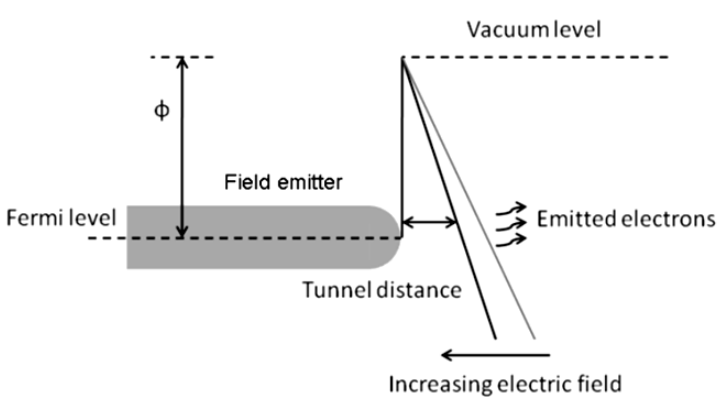

Fowler-Nordheim Law

$$J_{FN} = a \cdot \frac{\beta^2 \cdot E^2}{\phi} \cdot e^{\frac{-b \cdot \phi^{1.5}}{\beta \cdot E}}$$

Field enhancement factor

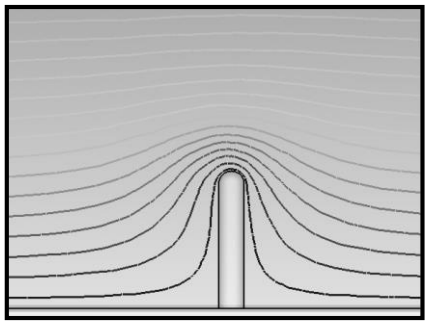

The Fowler and Nordhiem function can be written isolating a multiplication factor, the Field Enhancement Factor β that can be increased by using carbon nanotubes. The main advantage of using cold cathode are the possibility of working at ambient temperature, the cathode patterning, small dimensions and the possibilility of modulate the emitted current

Operative principles

Vacuum Electron Gun

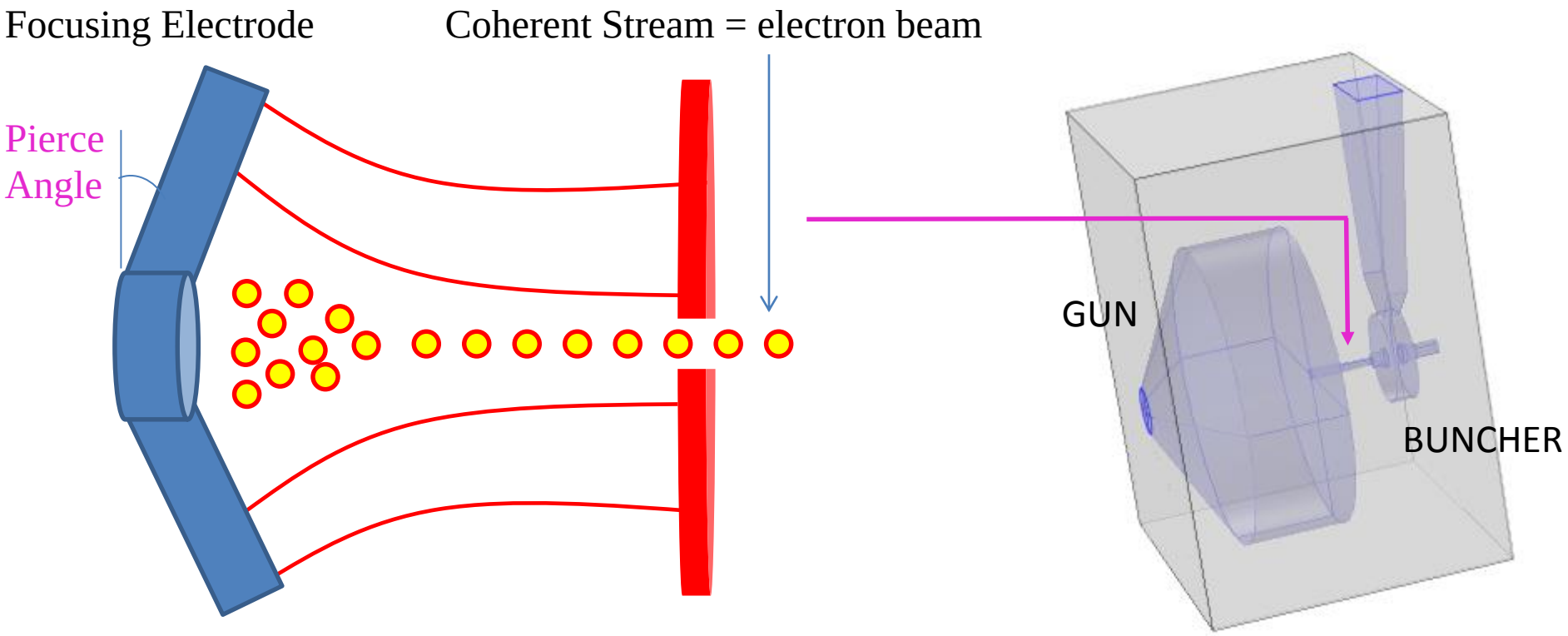

By opening a hole in the anode, electron can escape from the anode representing a coherent stream, the electron beam. A beam consists of particles with the same energy and direction (with a distribution). This beam can be employed in more complex electron tubes that need such a coherent stream as principal electron flux to manipulate.

Operative principles

Klystron

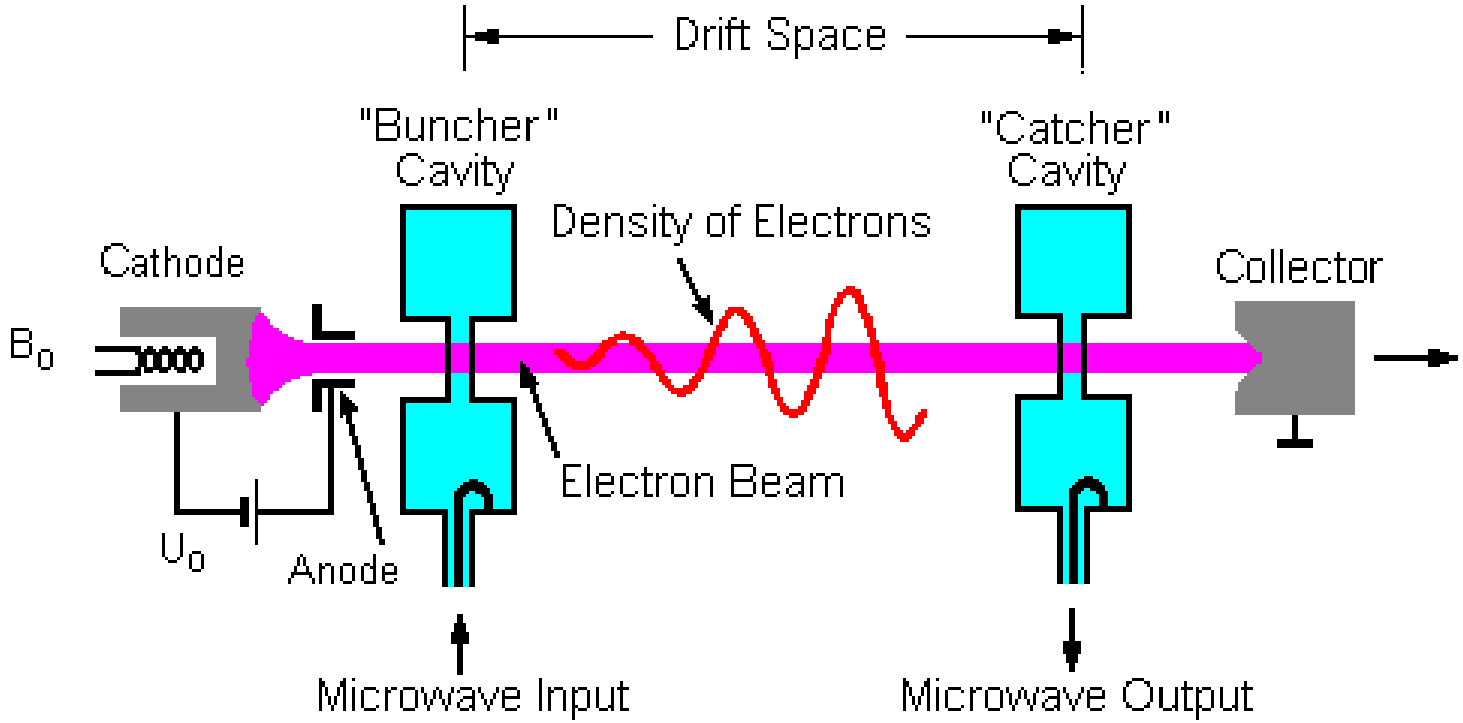

In a Klystron, the electron beam produced by an electrostatic gun, first interacts with the Buncher cavity, where undergoes the force a low energy alternate field that modulates the electron velocity. As the beam has crossed an opportune distance from the Buncher, the velocity modulation become a modulation of the charge density and the beam, forwarded in another cavity, induces an oscillating field stronger than the first. Finally, the beam is collected at the anode. These dynamic results in an amplification of the signal. Since no magnetic field is required, klystrons are good candidates for micro vacuum tube realization

Operative principles

Buncher Cavity of the Klystron

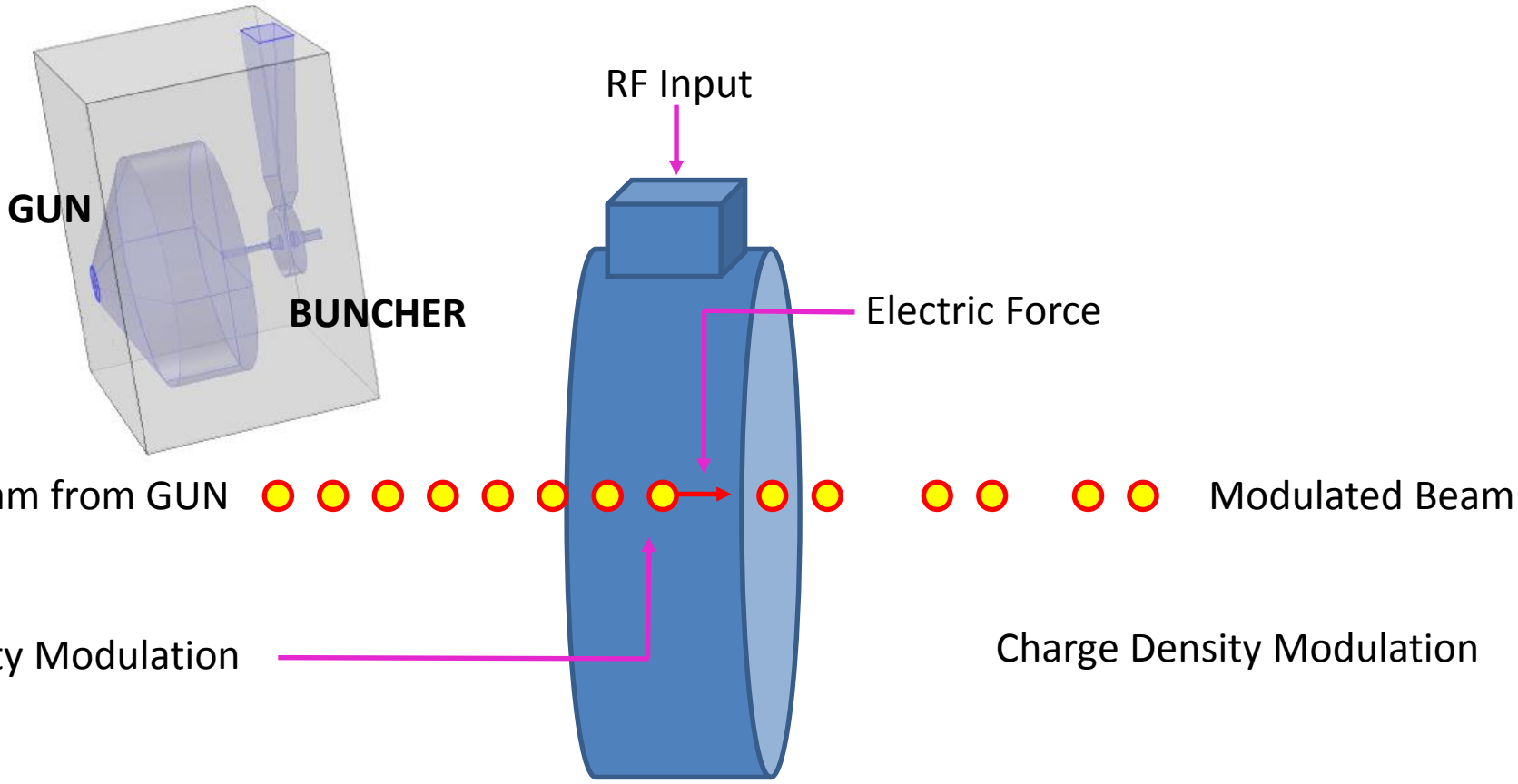

The RF field produces the axial electric field in the Buncher to impress forces to the electrons, in order to modulate their velocity. Correct operation of the Buncher is ensured if it can use all the available power provided at the input to produce the desired axial electric field (bunching field). The Buncher needs to be critically matched to the RF source at the working frequency.

Operative principles

Thermal dependance of Frequency of Resonance

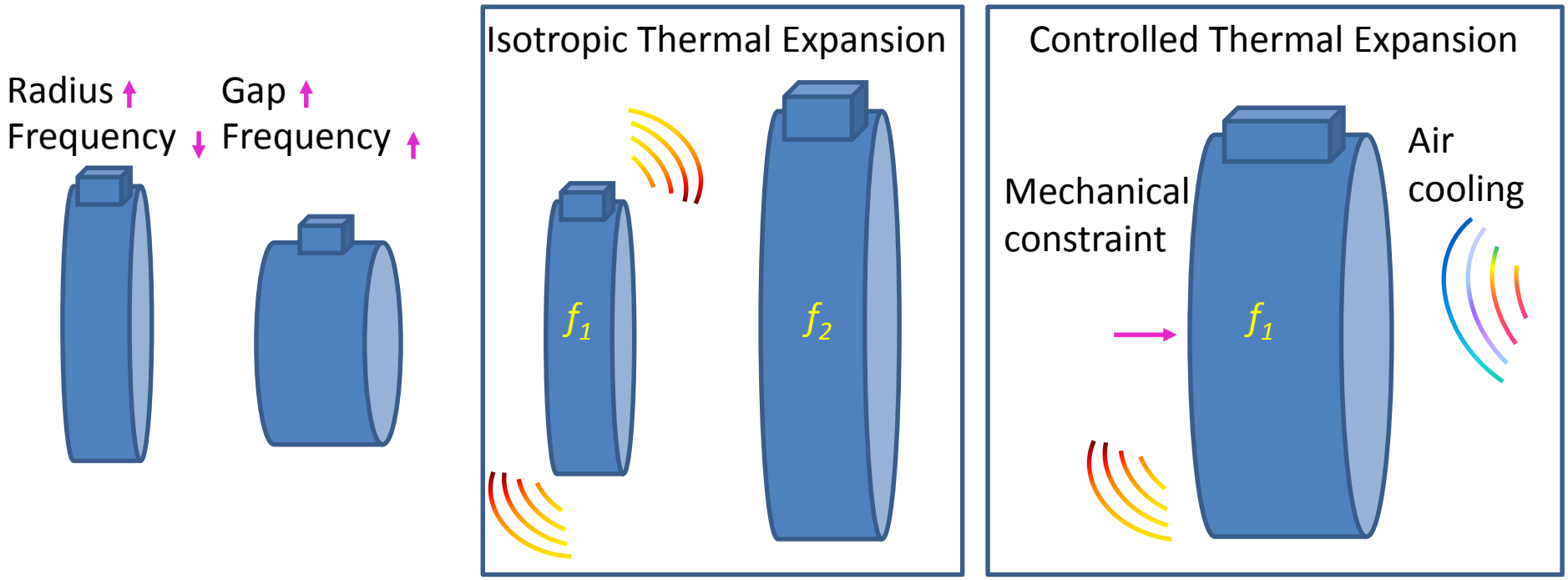

The Buncher has the shape of a reentrant cavity: Typically, if the cavity radius is increased, the resonance frequency decreases and, albeit often with less effect, if the cavity gap increases the frequency increase. An isotropic thermal expansion may dilate the cavity Buncher mainly decreasing the operative frequency. This effect can be compensated by decreasing the surrounding temperature, requiring important cooling systems. In the proposed application, mechanical constraint and possible direction of thermal expansions have been considered, in order to obtain the desired compensation of the frequency lowering.

Outline

- Introduction
- Operative principles
- Motivations
- Buncher Features
- Numerical model
- Simulation Results
- Conclusions

Motivations

Multiple Physics Influencing Factors

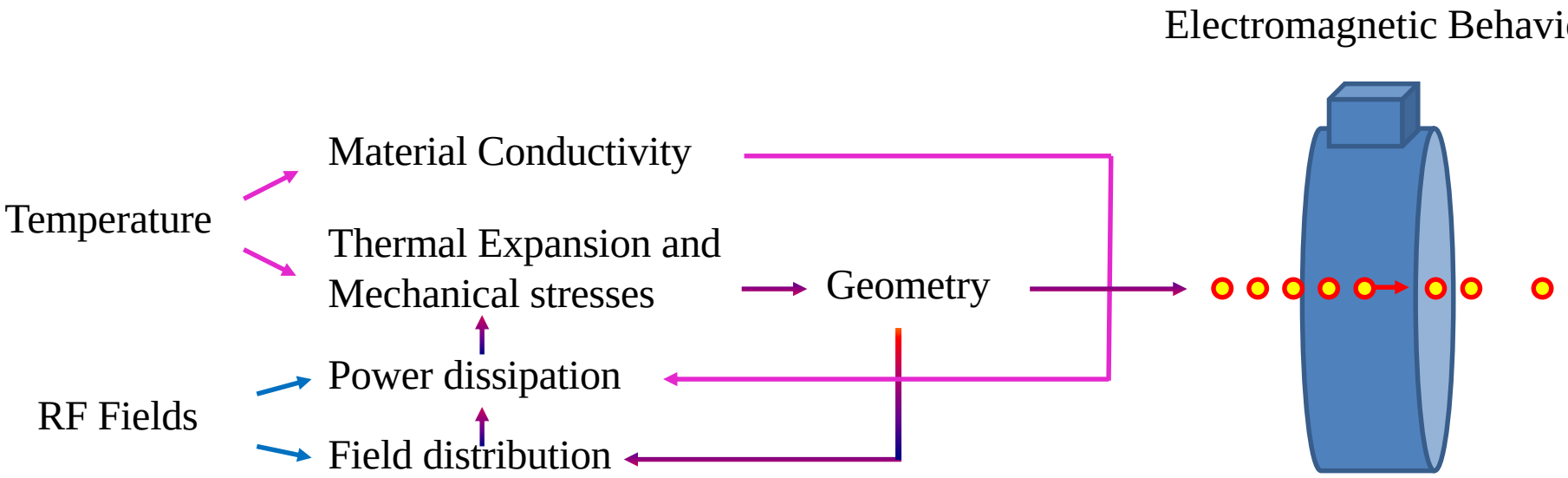

Critical operation in small dimension Range

An uncontrolled thermal expansion may produce destructive effects over the desired beam dynamics. This study proposes the analysis of the Buncher cavity of the klystron while it experience the heating effects of its power dissipations, due to the wall current, and the electron gun closely connected.

Motivations

Multiphysics Simulation Ambient

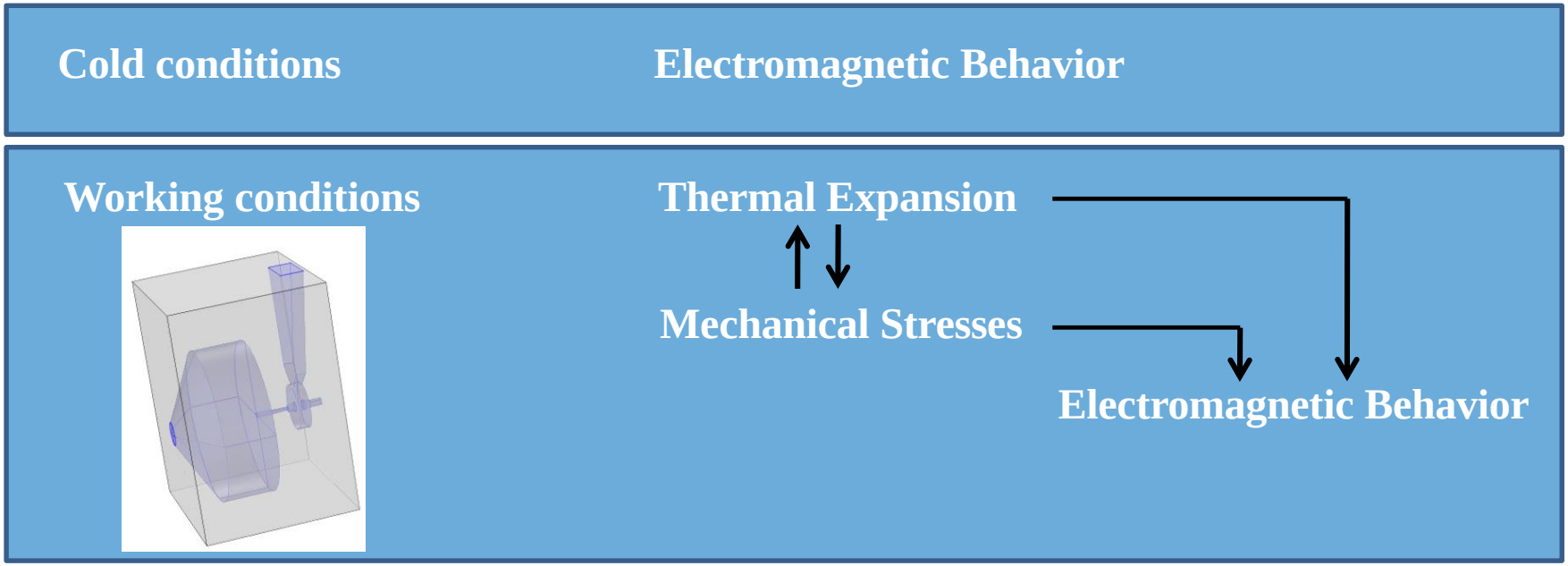

The analysis follows a Multiphysics model approach, in order to prevent alterations of the electromagnetic (EM) behavior, while exposing the device to these multiple physics factors. By a Thermo-mechanical (TM) analysis, temperature and deformation have been determined considering the heating effects due to the resonator power dissipation superposed to that of the cathode, when whose heat flux has been diffused on all the reachable components, cooled externally by an opportune airflow.

Outline

- Introduction
- Operative principles
- Motivations
- Buncher Features
- Numerical model
- Simulation Results
- Conclusions

Buncher Features

Buncher Model

Electron Gun: I_b= 16 mA, E_b=10 keV, r_b=100µm

Buncher: P_{in}= 1 W, f = 131.68 GHz, RL=21 dB, Z_S= 342.5 kΩ

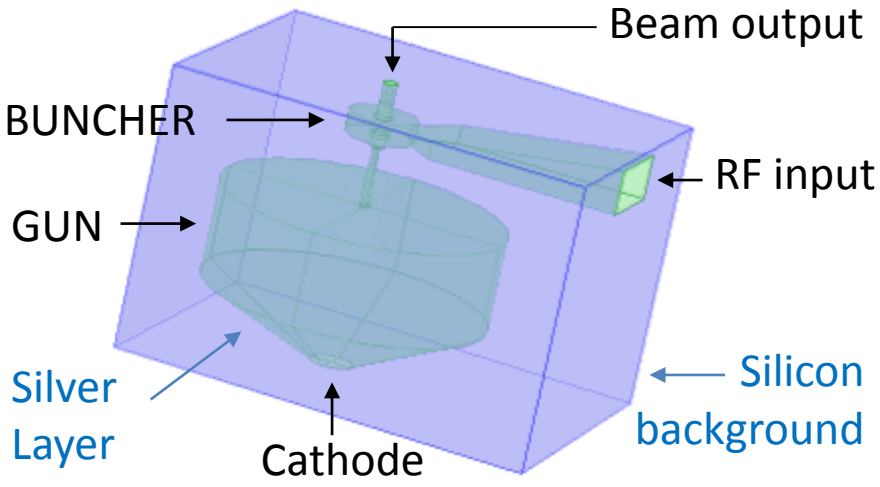

The solid material is a block of Silicon at which interior, the vacuum region of electron gun and Buncher is present. A layer of Silver is deposed on the internal surfaces except for the circular lateral surface of the gun that insulate the anode to cathode. Anode and cathode are made of molybdenum; the interaction region is made of non-ideal vacuum (air at 10^{-7} bar).

Outline

- Introduction
- Operative principles
- Motivations
- Buncher Features
- Numerical model
- Simulation Results
- Conclusions

Numerical model

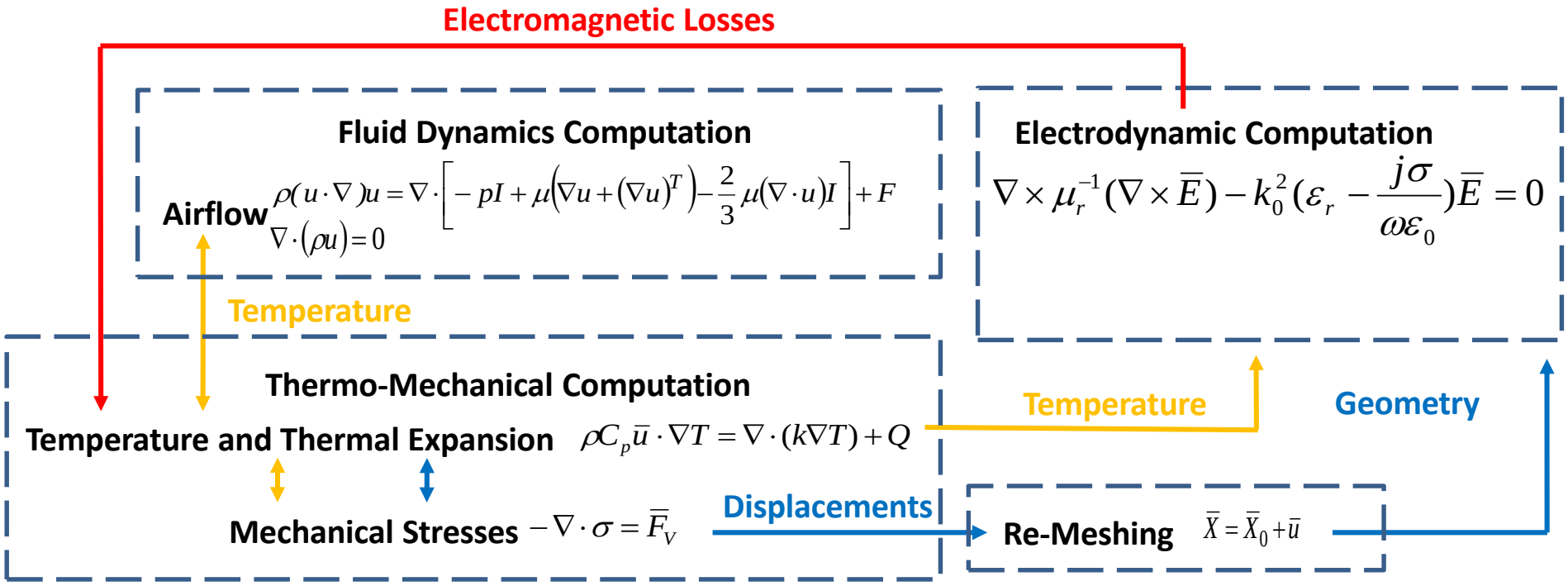

A Thermodynamic (TD) and Fluid Dynamic (FD) analysis have been coupled and the resulting temperature distribution and matrices of displacements is obtained. These displacements have been employed to obtain a deformed geometry by Moving Mesh (MM) dedicated interface and storing temperature information [10]. Electromagnetic analysis has been executed on the new meshes receiving the temperatures evaluated by the TD and FD studies. A first EM analysis has been employed to calculate the microwave power dissipations when wall current flows on the cavity walls while it receives the operative input signal (1 W mean power) at the input port. This power dissipation has been prescribed into the thermodynamic calculation as a heat power source.

Numerical model

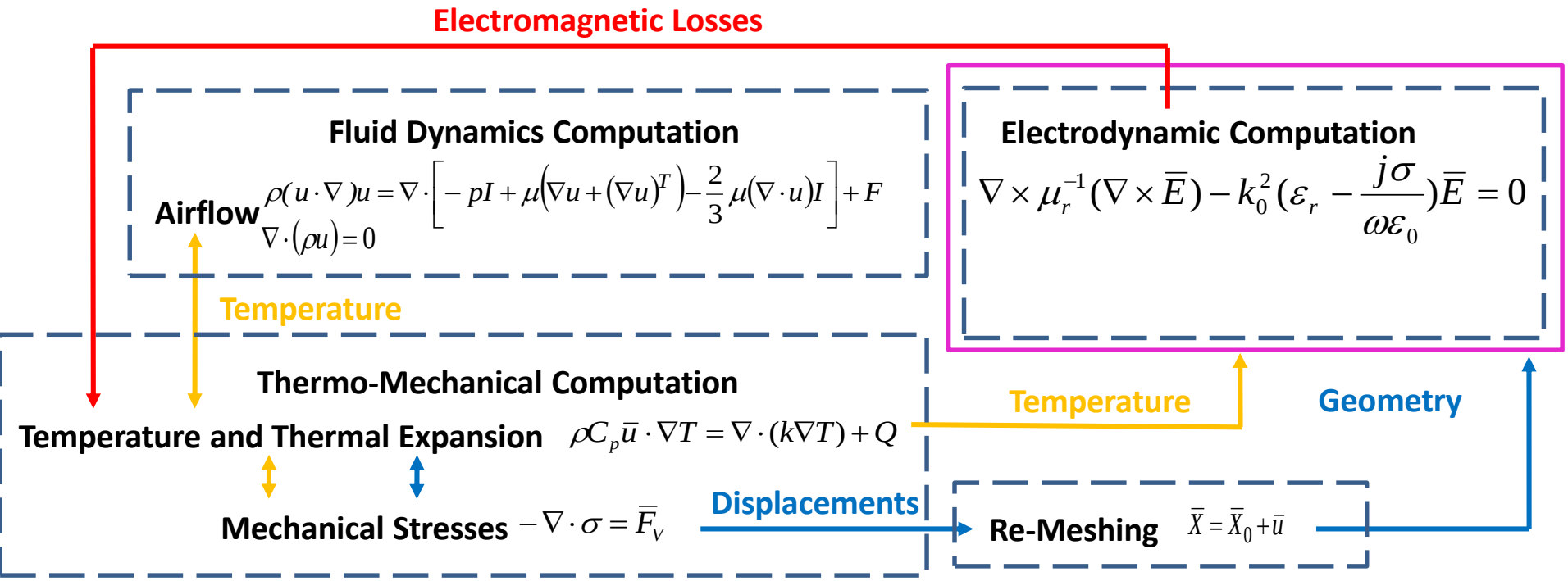

The preliminary EM analysis is the first step. It has been employed to calculate the microwave power dissipations when wall current flows on the cavity walls while it receives the operative input signal (1 W mean power) at the input port. This power dissipation has been prescribed into the thermodynamic calculation as a heat power source.

Numerical model

Electromagnetic Analysis

Multiphysics Simulation Ambient

Electromagnetic Analysis $$\nabla \times \mu_r^{-1}(\nabla \times \bar{E}) - k_0^2(\varepsilon_r - \frac{j\sigma}{\omega\varepsilon_0})\bar{E} = 0$$

In the formula: μ_r is the relative magnetic permeability, ε_r the relative electrical permittivity and σ the electrical conductivity of the material ($S \cdot m^{-1}$); ε_0 is the electrical permittivity of the vacuum ($F \cdot m^{-1}$), k_0 the wave number in free space (m^{-1}), ω the wave angular frequency (s^{-1}) and the electric field ($V \cdot m^{-1}$).

Numerical model

Electromagnetic Analysis

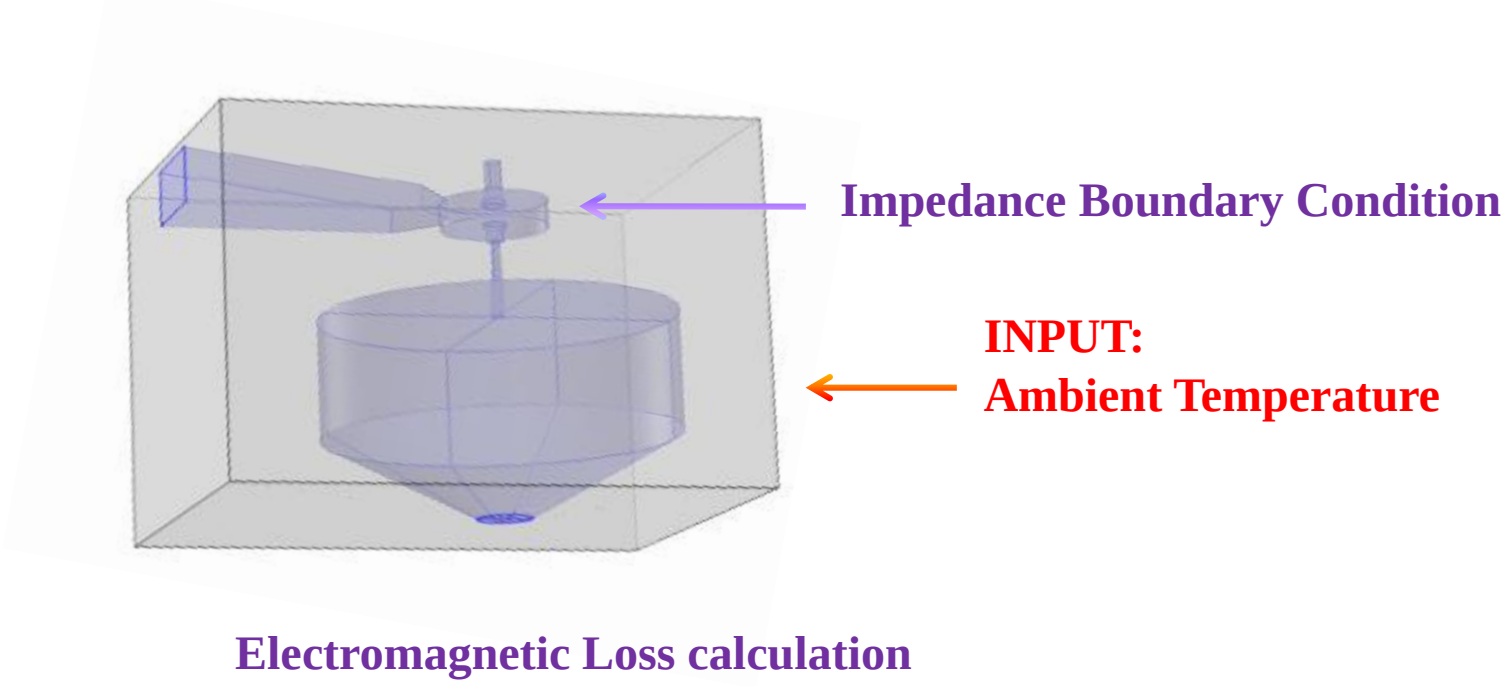

Impedance boundary condition: The surfaces, shared between vacuum and the supporting solid material, are modeled in order to consider the losses due to the partial penetration of the electric field in the lossy material which constitutes such walls. This condition allows to exclude a further domain to the EMW calculation, avoiding the meshing and saving computational cost. The specified thickness of the wall boundaries is fixed to 80μm. Electric conductivity is determined considering its thermal dependence basing on material properties.

Numerical model

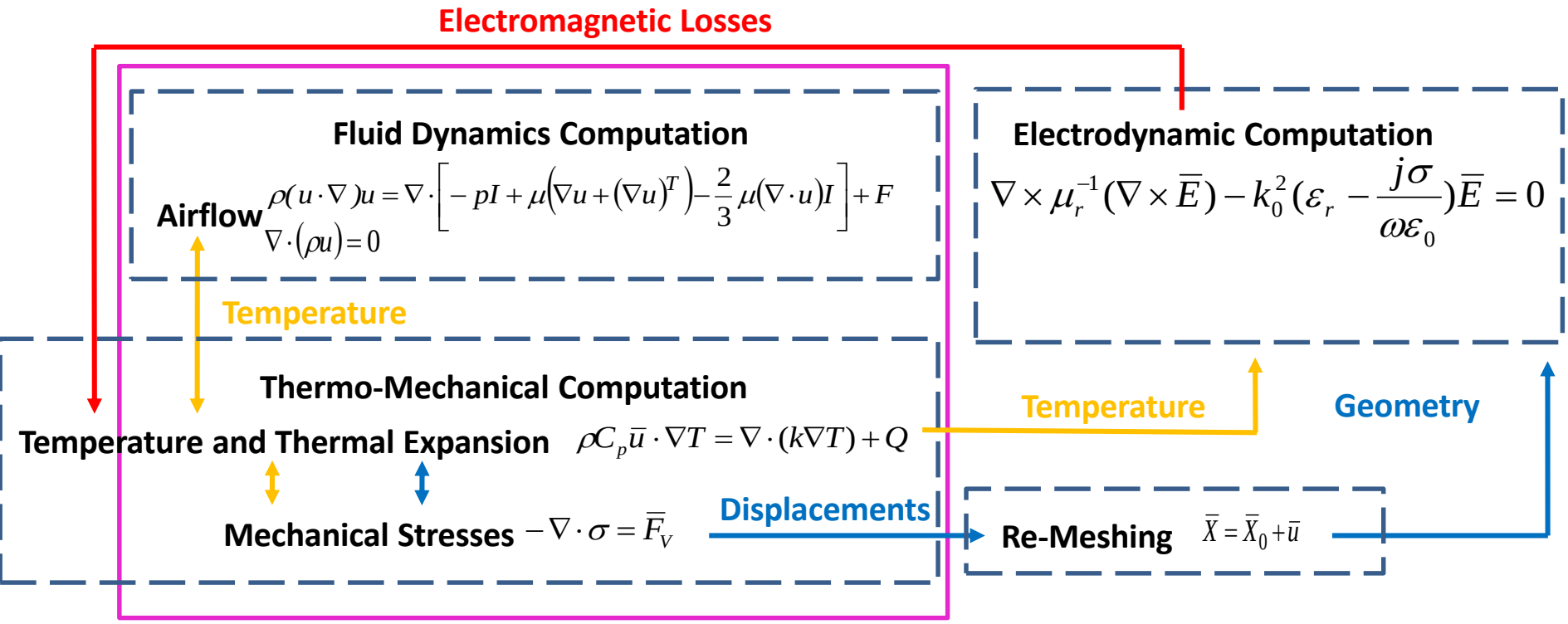

Thermo-mechanical with Fluid Dynamics Computation is the second step. The heat is computed in the whole volume, receiving in input the temperature on the emitting surface of the cathode (which is a figure of merit of the employed cathode).

Numerical model

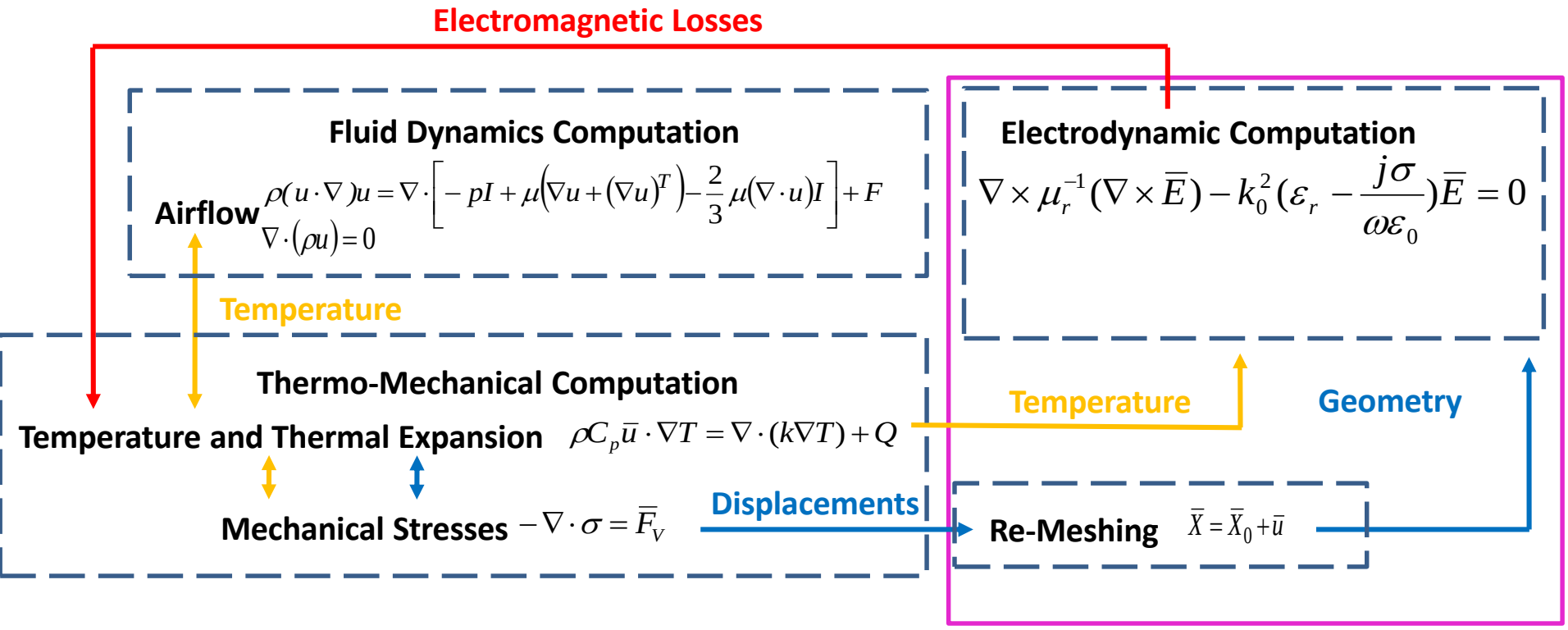

A Re-messhing of the geometry is performed: The displacements have been employed to obtain a deformed geometry by Moving Mesh (MM) dedicated interface.

Electromagnetic analysis is the last step. It has been executed on the new meshes receiving the temperatures evaluated by the TD and FD studies.

Numerical model

Thermo-mechnical and Fluid Dynamics Computation

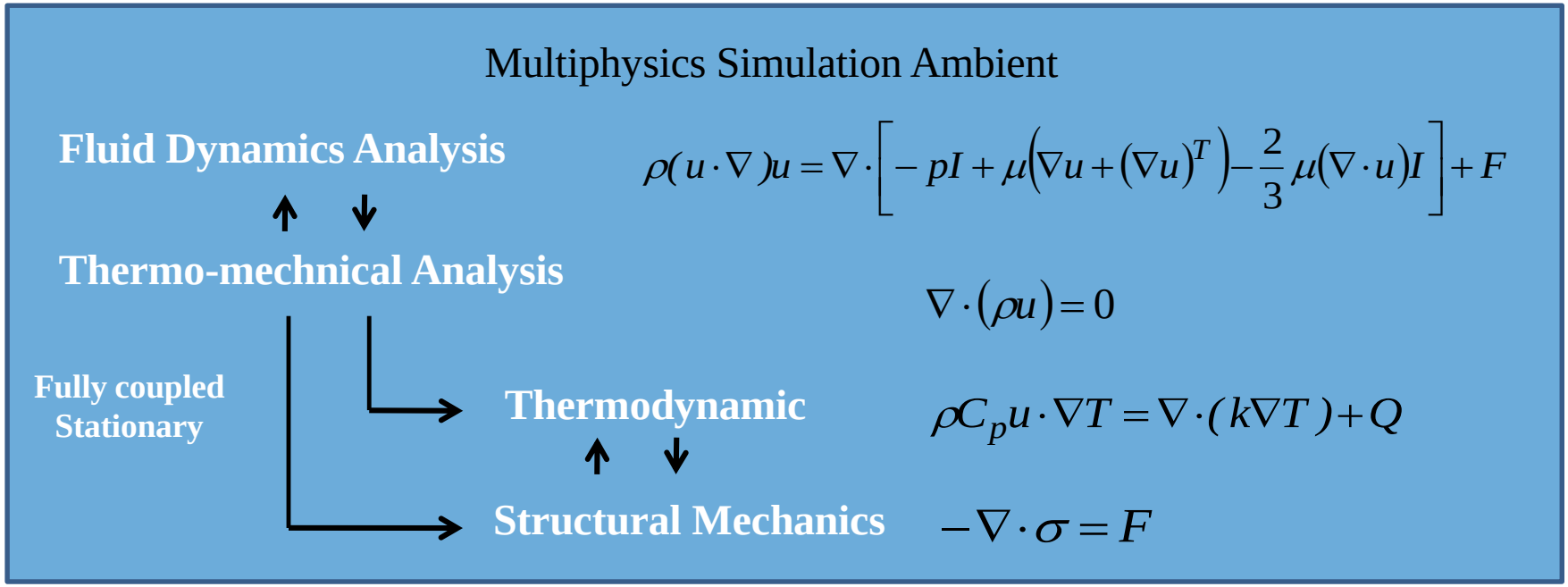

In the formulas: p is the pressure, μ the dynamic viscosity (Pa·s) of the material (the air) and F is the force per unit volume (N·m-3). The symbol I stand for the identity matrix and T for the transposing operation. The external environment temperature is Text = 25°C, σ is the stress ; ρ is the density, C_p the heat capacity at constant pressure, and k the thermal conductivity of the material. T is the temperature computed on the surfaces, Q is the heat source, u is the velocity field vector.

Numerical model

Thermo-mechnical and Fluid Dynamics Analysis

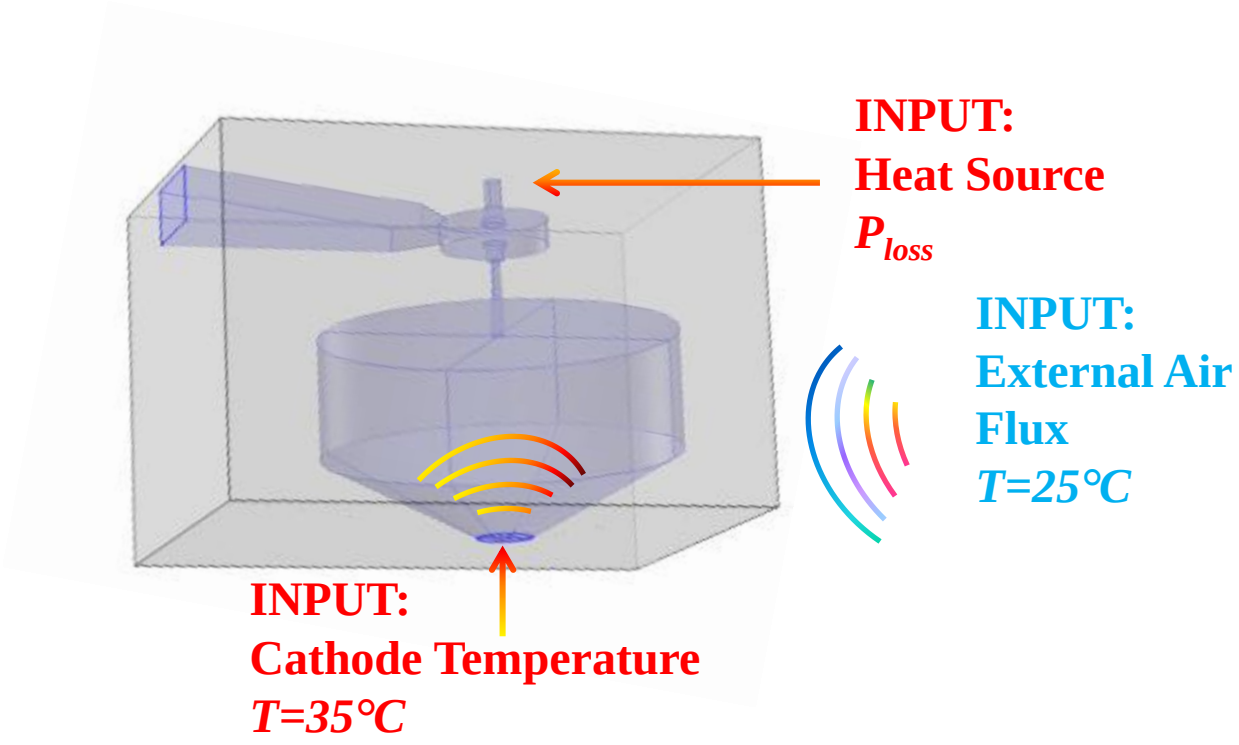

The structure is subjected to an air flow of 2 ms-1 velocity oriented towards the lateral surface, opposite to the side of the input flange. The external environment temperature is T_{ext} = 25°C, consistently with a typical environment temperature condition. The cathode surface has been considered at its nominal operative temperature that is 35°C. The power dissipation calculated in a preliminary Electromagnetic analysis has been prescribed on the Buncher walls as surface density power source

Numerical model

Thermo-mechnical and Fluid Dynamics Analysis

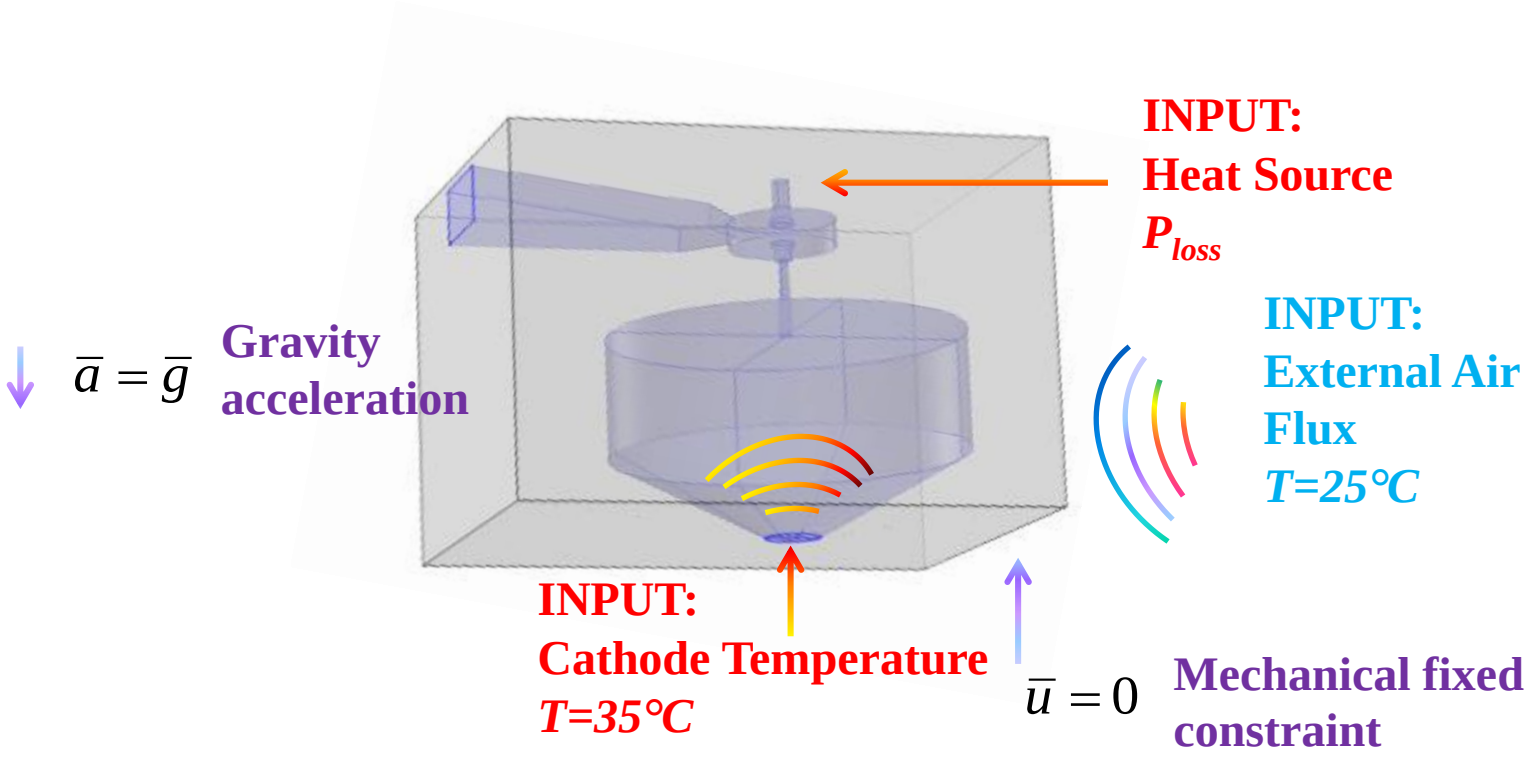

The external base surface of the cathode is locked to rigid structures in order to support the device. Thus, represents a mechanical fixed constraint. Gravity acceleration has been also considered.

Numerical model

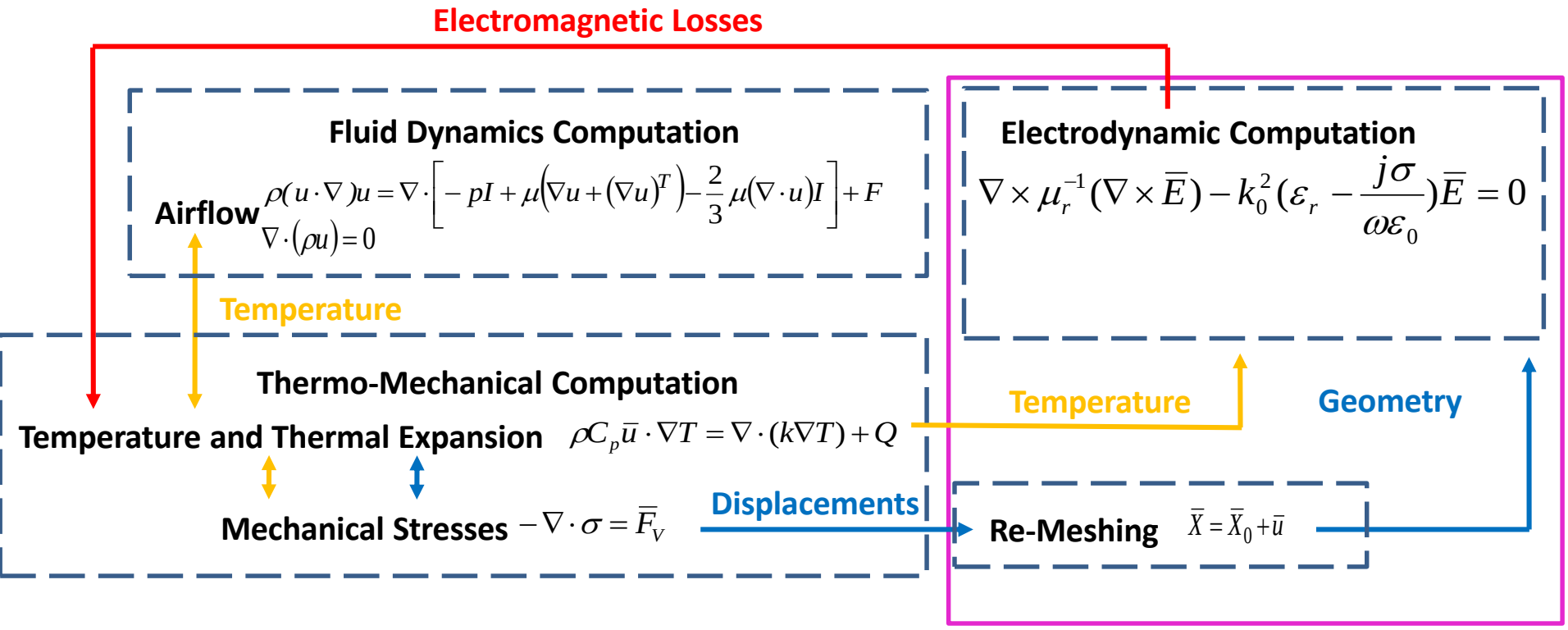

A Re-messhing of the geometry is performed: The displacements have been employed to obtain a deformed geometry by Moving Mesh (MM) dedicated interface.

Electromagnetic analysis is the last step. It has been executed on the new meshes receiving the temperatures evaluated by the TD and FD studies.

Numerical model

Mesh displacement computation

Applied to the whole structure.

$$\overline{X} = \overline{X}_0 + \overline{u}$$

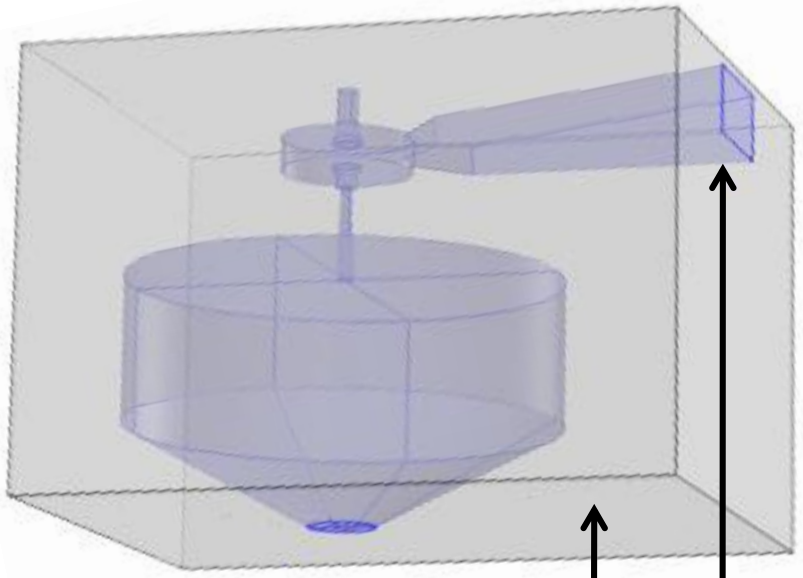

From TM

Volume prescribed Deformation → Silicon background
Volume Free Deformation → Non ideal vacuum
Surface Prescribed Mesh Displacement → Surfaces shared with background and the non ideal vacuum volume

Prescribed deformation: The structure of the gun and Buncher represent the volume subjected to deformation. The displacement vectors (u, v, w) computed by the SM module are employed to specify this volumetric deformation. Free deformation: The non ideal vacuum and air volumes (which are not subjected to any structural elastic formulation by the SM analysis) are free to move. Mesh Displacement: This condition specifies that the surface boundaries shared between the volumes subjected to deformation and the ones free to move need to be deformed by the SM computation.

Numerical model

Electromagnetic Analysis

Multiphysics Simulation Ambient

Electromagnetic Analysis $$\nabla \times \mu_r^{-1}(\nabla \times \bar{E}) - k_0^2(\varepsilon_r - \frac{j\sigma}{\omega\varepsilon_0})\bar{E} = 0$$

In the formula: μ_r is the relative magnetic permeability, ε_r the relative electrical permittivity and σ the electrical conductivity of the material ($S \cdot m^{-1}$); ε_0 is the electrical permittivity of the vacuum ($F \cdot m^{-1}$), k_0 the wave number in free space (m^{-1}), ω the wave angular frequency (s^{-1}) and the electric field ($V \cdot m^{-1}$).

Numerical model

Electromagnetic Analysis

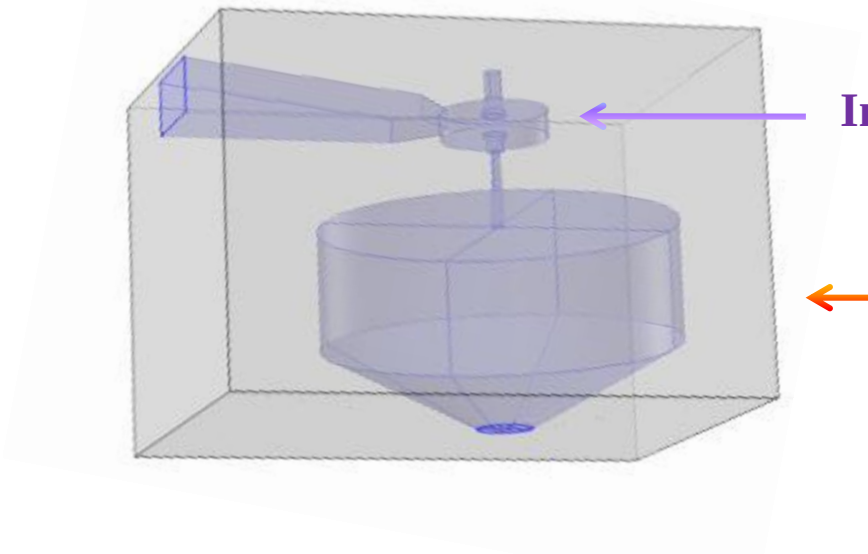

Impedance Boundary Condition

INPUT:
Temperature from TM Computation

Scattering Parameter and Electric Field Calculation

Impedance boundary condition: The surfaces, shared between vacuum and the supporting solid material, are modeled in order to consider the losses due to the partial penetration of the electric field in the lossy material which constitutes such walls. This condition allows to exclude a further domain to the EMW calculation, avoiding the meshing and saving computational cost. The specified thickness of the wall boundaries is fixed to 80μm. Electric conductivity is determined considering its thermal dependence basing on material properties.

Outline

- Introduction
- Operative principles
- Motivations
- Buncher Features
- Numerical model
- Simulation Results
- Conclusions

Simulation Results

Thermomechanical features

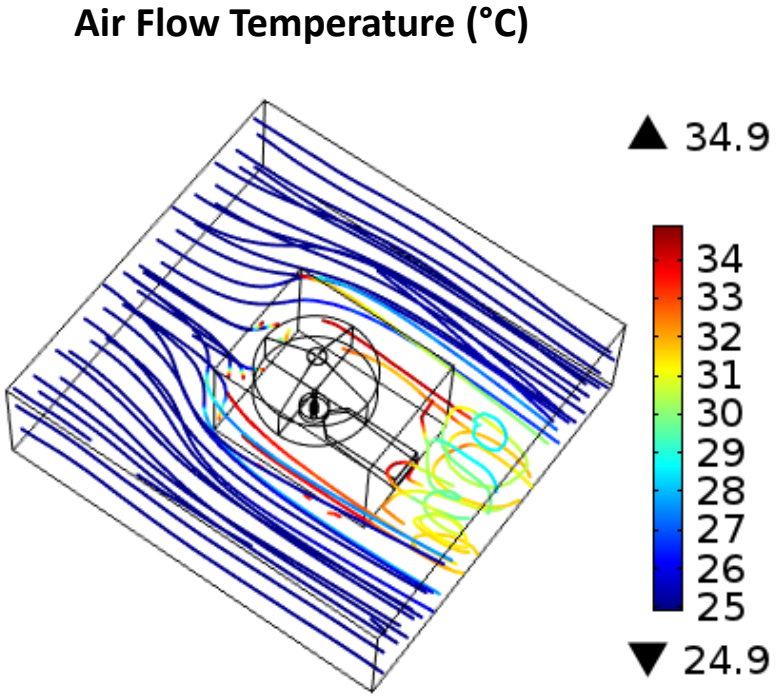

While the airflow enters the box, it is at this temperature, and then by exchanging heat with the device external surface, it becomes warmer approaching to a maximum temperature of 34.9°C, when it hits the device. This is the needed effect that allows to contain the dilation of the cavity radius.

Simulation Results

Thermomechanical features

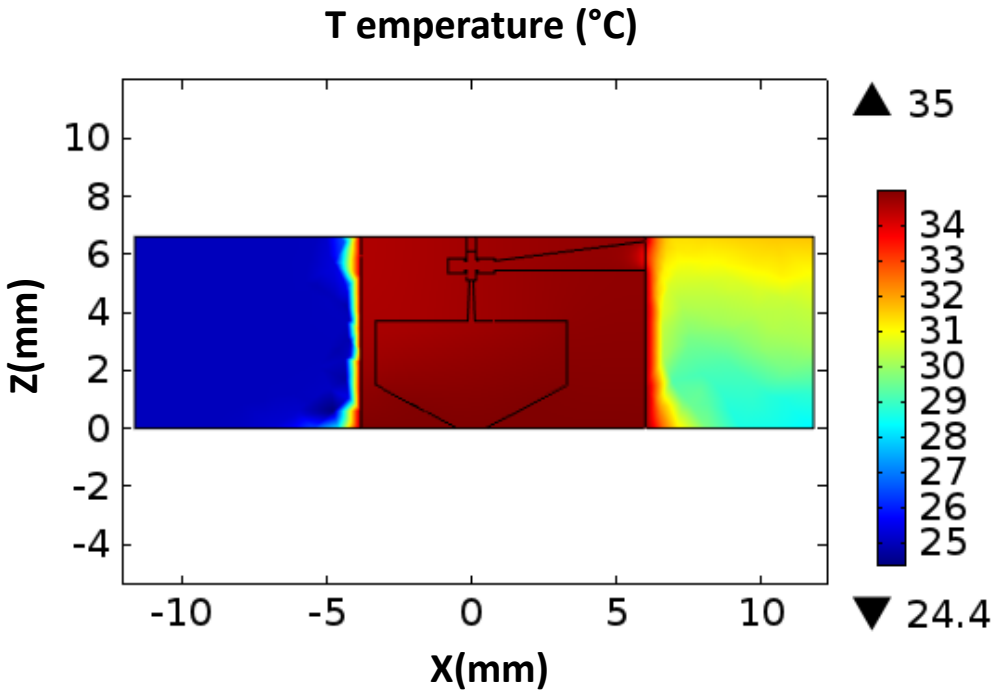

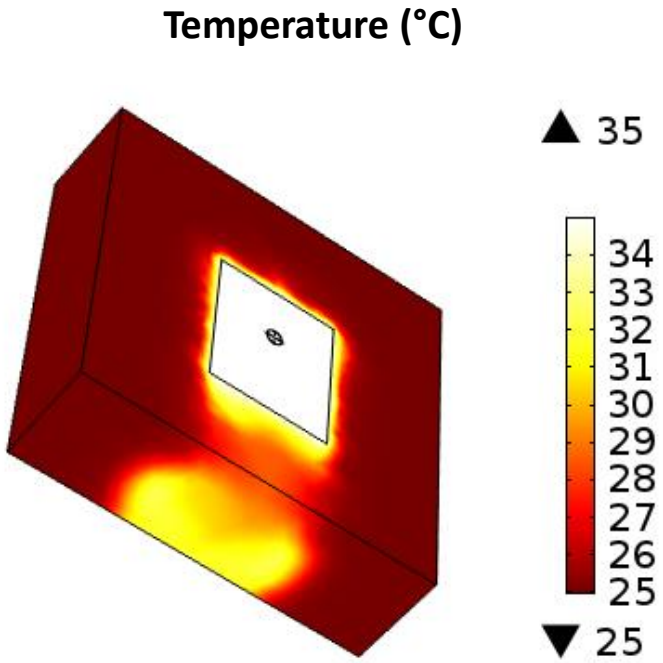

The maximum temperature reached internally is 35°C. This is due to the cathode operative temperature at the lower surface.

Simulation Results

Thermomechanical features

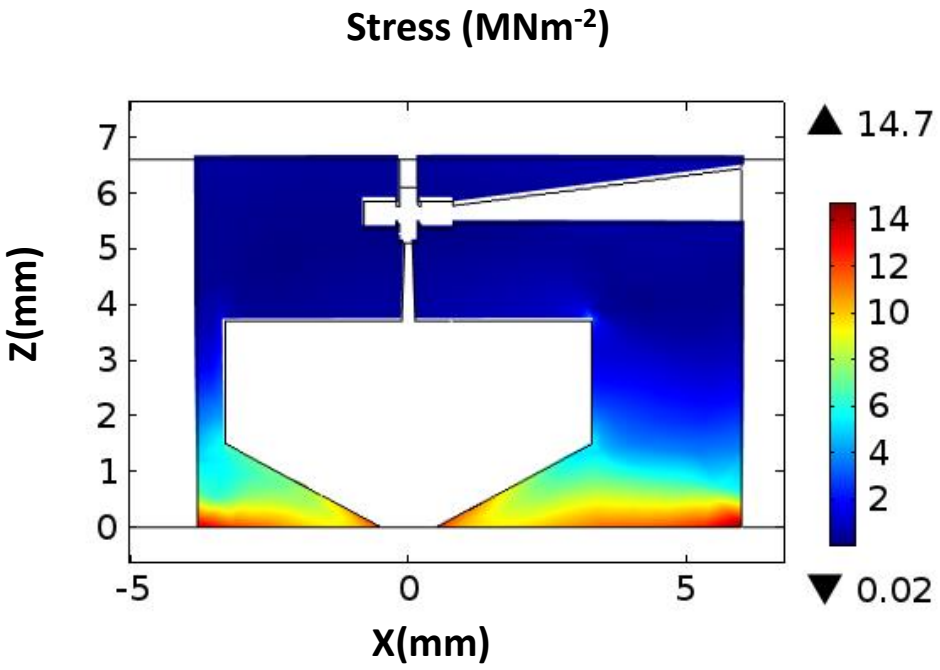

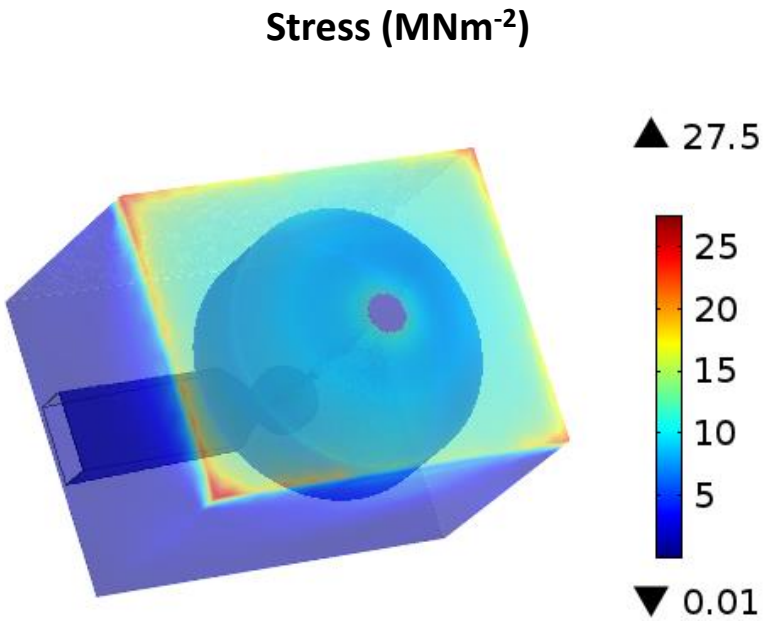

The maximum stress is about 27.5 MNm^{-2} located at the edges of the warmest face which is fixed to the rigid support. This is due to the high stiffness of silicon that counteracts the binding forces at the fixed surface.

Simulation Results

Thermomechanical features

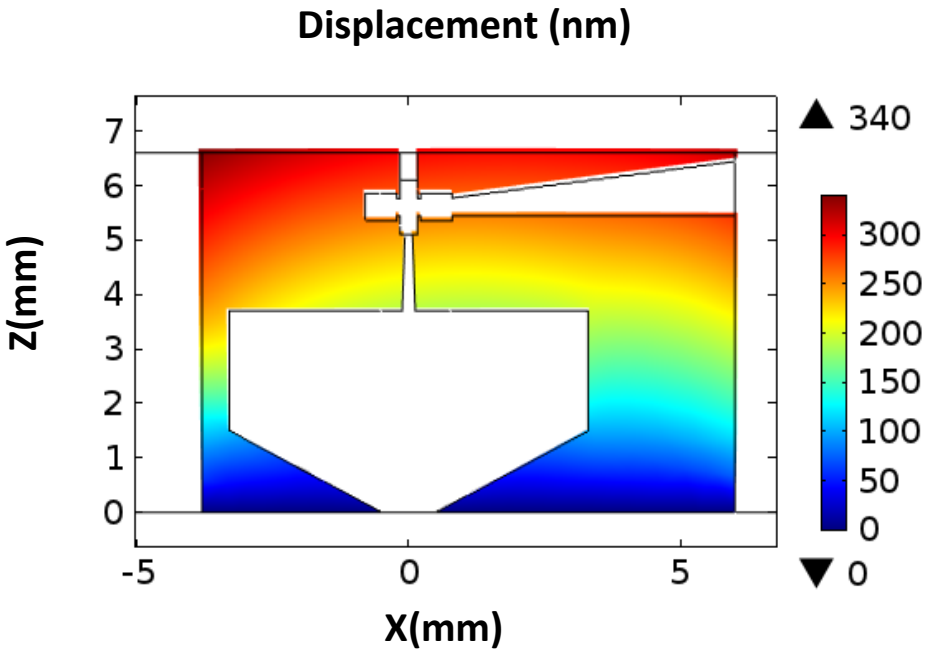

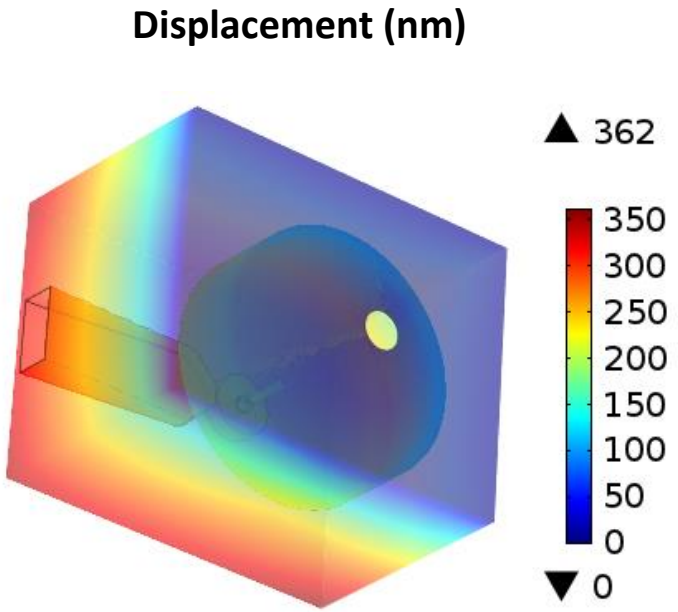

The internal shape, more free to deform, is less stressed, farther from which, the maximum total displacement is and is about 362 nm (due to the low thermal expansion of silicon and to the fact that this face is at 25°C, only 5°C more than the reference temperature). It can be also noted the achievement of the desired displacement: More displacement is directed along the axial direction *z* and less along the radial direction *x*.

Simulation Results

Electromagnetic Features

E dynamic Field (MVm^{-1}) Cold

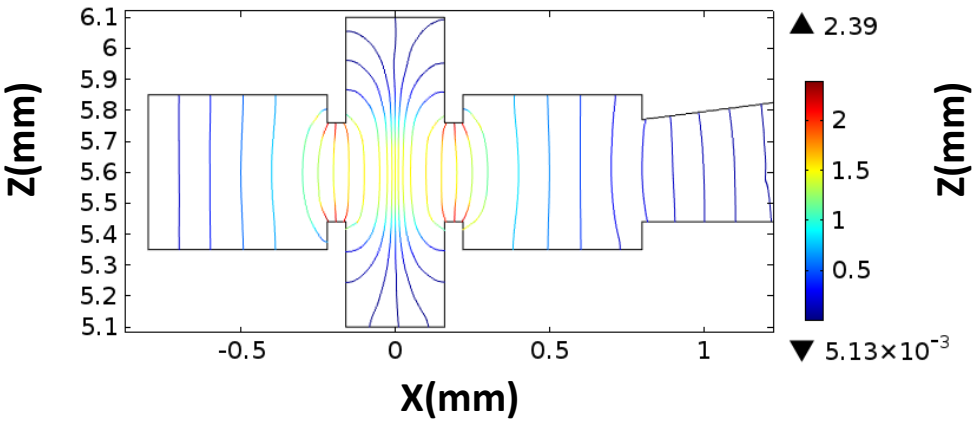

E dynamic Field (MVm^{-1}) Operative

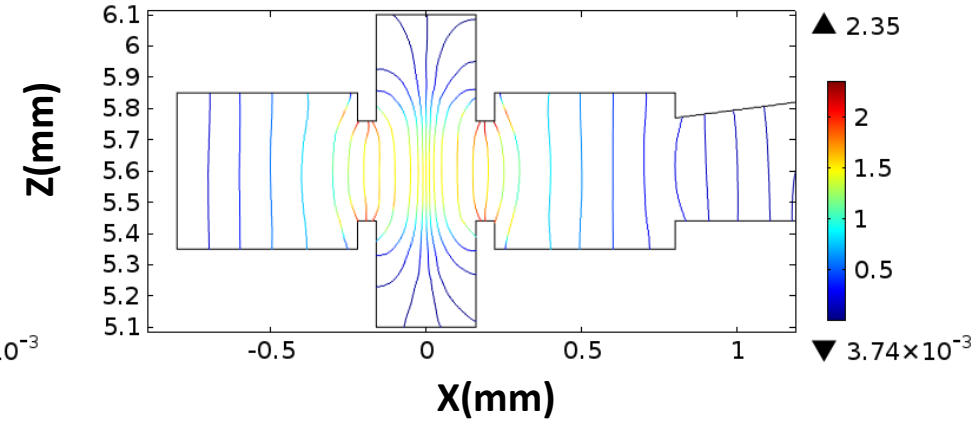

The streamline distribution of the electrodynamics fields for the bunching along the central plane are reported. In cold and in thermo mechanical operating conditions respectively E_{ACmax} = 2.39 and E_{ACmax} = 2.99 MVm^{-1} are reached. It can be noted that these fields are distribute in the pattern of the desired resonant mode, the quasi TM_{010} expected

Simulation Results

Electromagnetic Features

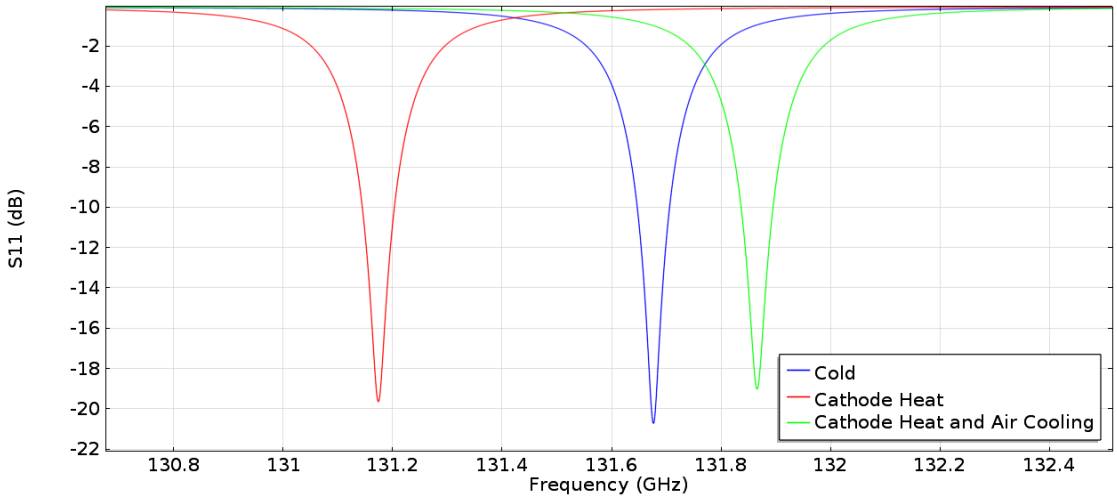

The scattering parameters in cold and in TM operating conditions have been documented In this analysis has been also considered the case of thermal insulation of the device. In this situation the device reaches a thermal steady state at the cathode temperature of 35°C, causing an isotropic thermal expansion that produces a considerable frequency lowering. This effect may happen if the system were enclosed in an insulated box, a situation preferably to be avoided but note. The dilation of the Buncher radius produces a dilation of the resonance wavelength, hence a frequency decreasing occurs. As shown in the red curve, the resonance frequency of the Buncher from the cold condition (where it has the value of f_1 = 131.68 GHz) decreases to f_2 = 131.17 if only the thermal heating is present without cooling air flux. In this condition a difference of 510 MHz can be noted between the two frequencies.

Simulation Results

Electromagnetic Features

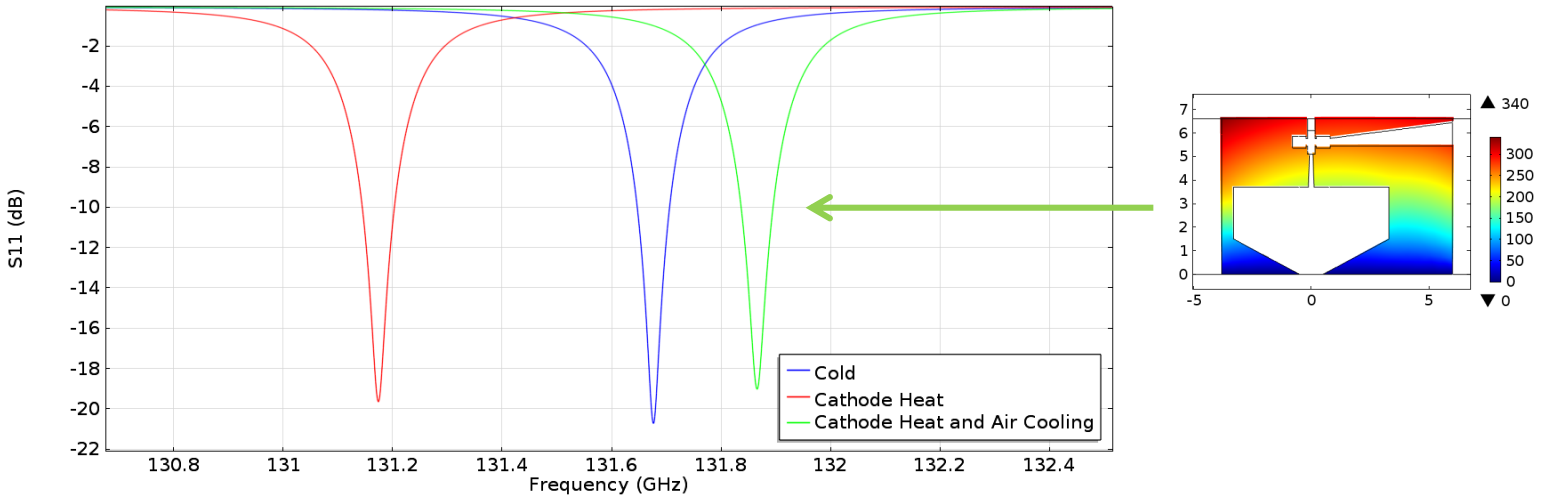

While the cooling air flux is operating, the controlled temperature at the Buncher lateral surfaces contains its shape alteration. Anyhow, the base surface, where the beam output hole is located, tends to expanse straightly, since is less refrigerated, due to the positioning of the air flux streamlines which are crossed to longitudinal axis of the Buncher. This effect allows for a frequency increase, as shown in the green curve, because the cavity gap is dilated. In this condition, the resonance frequency moves to f_3 = 131.87. The return loss decrease from 18.7 to 18.4dB. This is a very small disadvantage if is compared to the advantage obtained over the frequency shift, which is decreased to 190 MHz, as discussed in the following text while treating the bunching field amplitude variation. It's evident as an opportune exterior shape can re-increase the performance of the device while it undergoes the operative influencing factors.

Simulation Results

Power Coupling

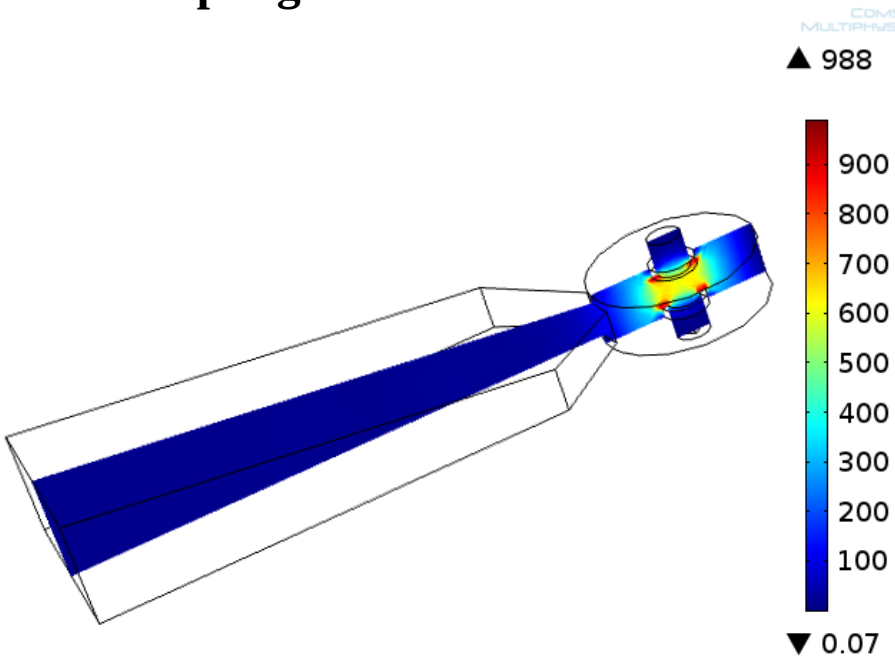

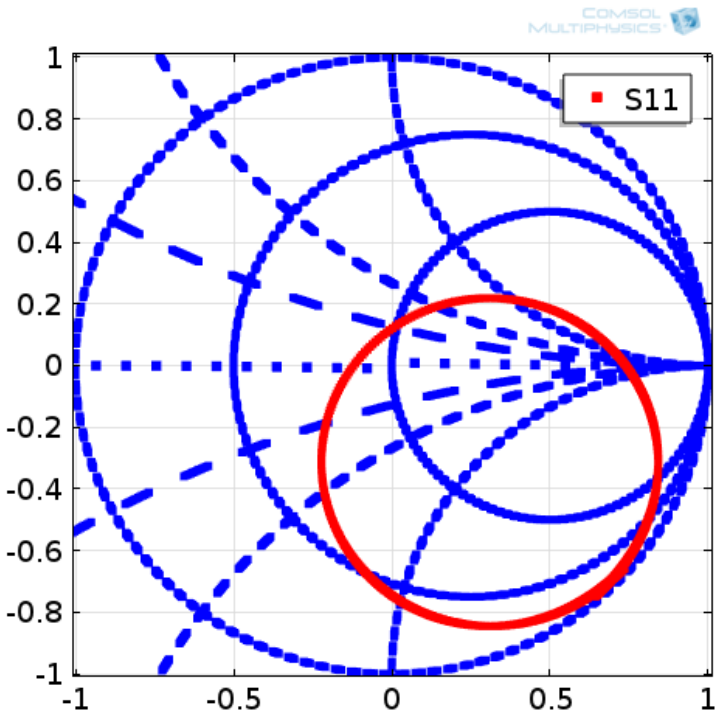

In order to evaluate the coupling between the cavity and the waveguide was useful to create a Smith chart on COMSOL. Since it is not present among the default plot menu, the Nyquist plot has been used with particular settings. Points of the Smith chart have been represented in function of the frequencies which compose the sweep for the analysis as the argument of exponential functions with different radii and centers. The Smith chart over the Nyquist plot is used to represent the scattering reflection parameter. The resonance tends to the critical coupling, as can be noted from the radius of the resonance circle which approaches to the unitary circle.

Simulation Results

Electromagnetic Features

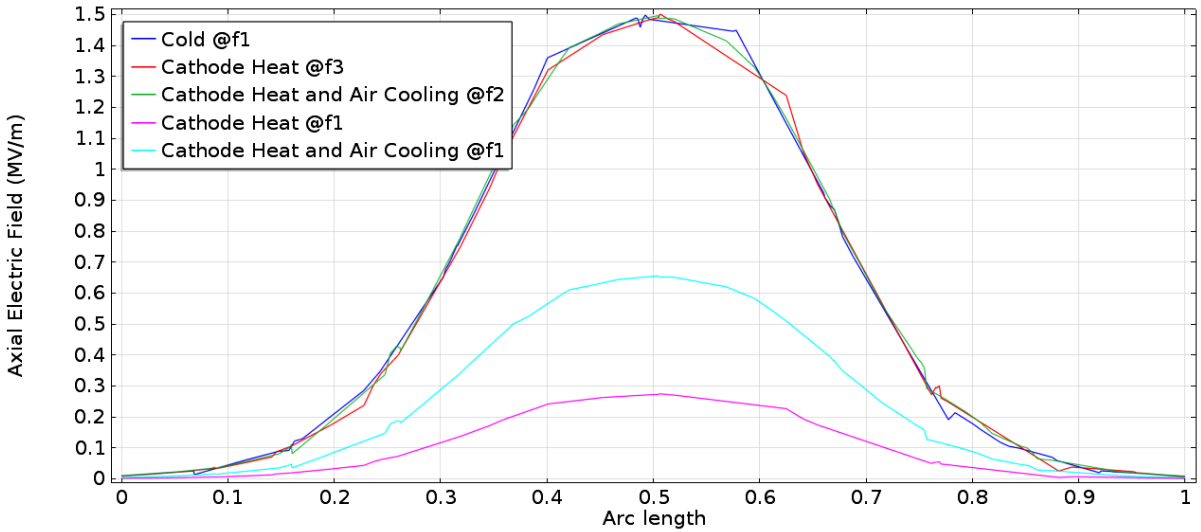

The longitudinal distribution of the electrodynamics bunching fields in cold and in thermo mechanical operating conditions is reported. In this analysis, in addition to the case of considering the sole cathode temperature without airflow, another effect has been highlighted: If the resonance frequency changes, is opportune to change the resonance frequency of the load (typically a resonant device) connected to the Klystron in order to transfer the maximum power also in operative conditions. If the load operates at f_1 while the Klystron is operating to f_2 or f_3 due to the TM alterations, to the load a poor power can be transferred, since the bunching field at the cold frequency is reduced to less than an half (see cyan curve). If the load is tuned to follow the operative frequency of the Klystron, the transferred power remains the same even if the frequency is shifted.

Outline

- Introduction
- Operative principles
- Motivations
- Buncher Features
- Numerical model
- Simulation Results
- Conclusions

Conclusions

The **Multiphysics design of a 130 GHz klystron Buncher** is described in this prewsentation. In order to reduce thermal expansion of the material typical of the classical thermionic cathodes, a Carbon nanotube cold cathode is employed.

A multiphysics design approach has been employed to ensure the future correct operation: **Temperature and deformations** have been determined when the heat generated by the cathode power dissipation has been diffused to the system, cooled by an opportune **airflow**.
Scattering parameters at the input port and **axial electric field** of the Buncher cavity have been calculated.

As demonstrated from this model, the silicon background material using cold cathode and cooling airflow **inhibits destructive thermal effects**.

In this study, has been shown a **strategy to allow for a frequency shift compensation** through the control an anisotropic thermal expansion, placing airflow in an opportune direction to cool some surface instead of others.

Several strategies have been adopted to obtain a simple but reliable model and the proposed approach has allowed to select the **appropriate materials and shapes**.

References

1. D. Passi, A. Leggieri, F. Di Paolo, M. Bartocci, A. Tafuto, A. Manna, “High Efficiency Ka-Band Spatial Combiner”, Advanced Electromagnetics, Vol. 3, No. 2, 2014, pp. 10-15. ISSN: 2119-0275.
2. N. Fourikis "Transmit/receive modules" in Advanced Array Systems, Applications and RF Technologies, Academic Press, London, UK, 2000, pp. 308-311.
3. Y. Xu and R. Seviour, “Design of Photonic Crystal Klystrons”, Proc. of IPAC'10,Kyoto, Japan, 2010, pp. 4001-4004.
4. Z.Zhibin and K.W. Zieher, “Design aspects of a 94 GHz extended interaction Klystron”, IEEE International Conference on Plasma Science, Madison, WI, USA, 5-8 June 1995.
5. M. Mineo and C. Paoloni, "Micro Reentrant Cavity for 100 GHz Klystron", IEEE Vacuum Electronics Conference (IVEC), Monterey, CA, 2012, pp. .65-66.
6. C. Paoloni, M. Mineo, H. Yin, L. Zhang, W. He, C.W. Robertson, K. Ronald, A.D.R. Phelps and A.W. Cross, "Scaled Design and Test of a Coupler for Micro-Reentrant Square-Cavities for Millimeter Wave Klystrons", IEEE Vacuum Electronics Conference (IVEC), Paris, 2013, pp. 1-2.
7. P.H. Siegel, A. Fung, H. Manohara, J. Xu, B. Chang, “Nanoklystron: A Monolithic Tube Approach to THz Power Generation”.
8. M. C. Lin, D. N. Smithe, P. H. Stoltz, H. Song, and T. Kalkur, “A Microfabricated Klystron Amplifier for THz Waves”, Proc. of IVNC 2009, pp. 189-190.
9. A. Leggieri, D. Passi, F. Di Paolo, B. Spataro and E. Dyunin, “Advanced Design of a Low Energy Electron Source”, Proc. of IEEE MTT-S International Conference on Numerical Electromagnetic and Multiphysics model and Optimization - NEMO, Ottawa, CA, 2015.
10. A. Leggieri, D. Passi, G. Felici, F. Di Paolo, “Multiphysics design of a Magnetron High Power Transfer System”. Proc. of IEEE EMS 2014 – European model Symposium, Pisa, 2014, pp. 466-472.
11. R. G. Carter, “Calculation of the Properties of Reentrant Cylindrical Cavity Resonators”, IEEE Transactions on Microwave Theory and Techniques, Volume 55, Issue 12, Dec. 2007.
12. J. R. Pierce, Theory and Design of Electron Beams, D. Van Nostrand Company, Canada, The Bell Telephone Laboratories Series, 1949.
13. COMSOL, “Heat transfer Module User’s Guide”, COMSOL AB, Stockholm, 2012, pp. 69-72,111-212.

COMSOL CONFERENCE 2015

UNIVERSITA' DEGLI STUDI DI ROMA TorVergata

Thank You !

Multiphysics Design of a Klystron Buncher

Alberto Leggieri, Davide Passi, Franco Di Paolo and Giovanni Saggio

Department of Electronic Engineering, University of Rome "Tor Vergata"
alberto.leggieri@uniroma2.it

EH Frontier
Expanding High-frequency Frontier

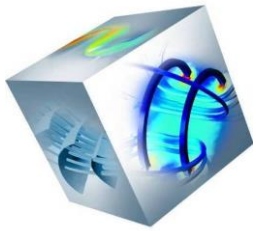

COMSOL